

**EXPERIMENTAL STUDY OF SOLVENT BASED EMULSION INJECTION TO
ENHANCE HEAVY OIL RECOVERY**

A Thesis

by

FANGDA QIU

Submitted to the Office of Graduate Studies of
Texas A&M University
in partial fulfillment of the requirements for the degree of

MASTER OF SCIENCE

May 2010

Major Subject: Petroleum Engineering

**EXPERIMENTAL STUDY OF SOLVENT BASED EMULSION INJECTION TO
ENHANCE HEAVY OIL RECOVERY**

A Thesis

by

FANGDA QIU

Submitted to the Office of Graduate Studies of
Texas A&M University
in partial fulfillment of the requirements for the degree of

MASTER OF SCIENCE

Approved by:

Chair of Committee,
Committee Members,

Head of Department,

Daulat D. Mamora
Ding Zhu
Zhengdong Cheng
Stephen A. Holditch

May 2010

Major Subject: Petroleum Engineering

ABSTRACT

Experimental Study of Solvent Based Emulsion Injection to Enhance Heavy Oil
Recovery. (May 2010)

Fangda Qiu, B.S., China University of Petroleum (Beijing)

Chair of Advisory Committee: Dr. Daulat D. Mamora

This study presents the results of nano-particle and surfactant-stabilized solvent-based emulsion core flooding studies under laboratory conditions that investigate the recovery mechanisms of chemical flooding in a heavy oil reservoir. In the study, bench tests, including the phase behavior test, rheology studies and interfacial tension measurement are performed and reported for the optimum selecting method for the nano-emulsion. Specifically, nano-emulsion systems with high viscosity have been injected into sandstone cores containing Alaska North Slope West Sak heavy oil with 16 API°, which was dewatered in the laboratory condition.

The experiment results suggest that the potential application of this kind of emulsion flooding is a promising EOR (enhanced oil recovery) process for some heavy oil reservoirs in Alaska, Canada and Venezuela after primary production. Heavy oil lacks mobility under reservoir conditions and is not suitable for the application of the thermal recovery method because of environmental issues or technical problems.

Core flooding experiments were performed on cores with varied permeabilities. Comparisons between direct injection of nano-emulsion systems and nano-emulsion

injections after water flooding were conducted. Oil recovery information is obtained by material balance calculation.

In this study, we try to combine the advantages of solvent, surfactant, and nanoparticles together. As we know, pure miscible solvent used as an injection fluid in developing the heavy oil reservoir does have the desirable recovery feature, however it is not economical. The idea of nano-particle application in an EOR area has been recently raised by researchers who are interested in its feature-reaction catalysis-which could reduce in situ oil viscosity and generate emulsion without surfactant. Also, the nano-particle stabilized emulsions can long-distance drive oil in the reservoir, since the nano-particle size is 2-4 times smaller than the pore throat.

In conclusion, the nano-emulsion flooding can be an effective enhancement for an oil recovery method for a heavy oil reservoir which is technically sensitive to the thermal recovery method.

DEDICATION

To my parents, Bo Qiu and Zhenyun Zhang

To Feng

ACKNOWLEDGEMENTS

I would like to express heartfelt gratitude to my committee chair, Dr. Daulat D. Mamora, for his support and guidance through my studies at Texas A&M University in the Department of Petroleum Engineering.

I am grateful for the experience I have gotten during the work on this research. I would also like to thank my committee members, Dr. D. Zhu and Dr. Z. Cheng, for their constant encouragement and academic support.

I am also thankful to my friends and colleagues and the department's faculty and staff for making my time at Texas A&M University an awesome experience.

I give my heartfelt appreciation to my parents, Mr. and Mrs. Qiu for their love and care throughout my childhood.

TABLE OF CONTENTS

	Page
ABSTRACT	iii
DEDICATION	v
ACKNOWLEDGEMENTS	vi
TABLE OF CONTENTS	vii
LIST OF FIGURES	x
LIST OF TABLES	xiii
1. INTRODUCTION	1
1.1 Overview of Alaska North Slope Heavy Oil	3
1.2 Main Challenges in ANS Heavy Oil Reservoirs	4
1.3 Chemical EOR in Developing Heavy Oil Reservoir	4
1.4 Objective.....	6
2. ENHANCED OIL RECOVERY-AN OVERVIEW	8
2.1 EOR Mechanism.....	10
2.2 Micro-emulsion and Macro-emulsion	12
2.3 Chemical EOR in Heavy Oil Reservoir.....	14
3. EXPERIMENTAL SET-UP AND PROCEDURES	18
3.1 Experimental Materials.....	18
3.1.1 Sandstone Core.....	18
3.1.2 Nitrogen.....	18
3.1.3 Crude Oil	18
3.1.4 Brine Solution	19

	Page
3.1.5 Surfactant	19
3.1.6 Nanoparticles	19
3.1.7 Solvent.....	19
3.2 Emulsion Bench Test Set-up and Procedure.....	20
3.2.1 The Phase Behavior Scan Set-up and Procedure	20
3.2.2 Emulsion Droplet Size Measurements	23
3.2.3 Surface Tension Measurements	24
3.2.4 Viscosity Measurements	25
3.2.5 Other Apparatus	26
3.3 Oil Dewatering Apparatus	28
3.4 Core Flooding Apparatus.....	29
3.4.1 Core Holder	30
3.4.2 Injection System.....	32
3.4.3 Production System.....	32
3.4.4 Data Logger System	32
3.5 Core Flooding Experiment Procedure	34
4. EXPERIMENTAL RESULTS AND DISCUSSION	36
4.1 Experimental Conditions	36
4.1.1 Bench Test Experimental Conditions.....	36
4.1.2 Core Flooding Experiment Conditions	36
4.2 Bench Test Experiments	37
4.2.1 Emulsion Phase Behavior Experiments.....	37
4.2.2 Emulsion Rheology Study Experiments	42
4.2.3 Emulsion and Crude Oil Interfacial Tension Measurement.....	46
4.2.4 Nanoparticle Thickened Micro-emulsion Experiments	48
4.2.5 Crude Oil Emulsion Viscosity Reduction Experiment	50
4.2.6 Core Flooding Experiments	52
4.2.7 Comparison of Experimental Results.....	70
5. SUMMARY, CONCLUSIONS AND RECOMMENDATIONS	74

	Page
5.1 Summary.....	74
5.2 Conclusions.....	74
5.3 Recommendations.....	76
REFERENCES.....	77
APPENDIX.....	79
VITA.....	82

LIST OF FIGURES

	Page
Fig. 1.1 Distribution of worldwide heavy oil resources	2
Fig. 1.2 Map of ANS area and distribution of oil extraction activities	3
Fig. 2.1 EOR target for different hydrocarbons	9
Fig. 2.2 The classification of enhanced oil recovery method.....	9
Fig. 2.3 Relationship between ROS and capillary number	11
Fig. 2.4 Comparisons between the two cases: $M > 1$ and $M \leq 1$	12
Fig. 3.1 The emulsion phase behavior experiments in the hood	21
Fig. 3.2 The microscope and the digital camera	23
Fig. 3.3 Kruss DSA30 IL4200 interfacial tension meter.....	24
Fig. 3.4 DV-III Ultra rheometer and the temperature control equipment	25
Fig.3.5 Ultrasound tub (left) and high speed range blender	26
Fig. 3.6 Centrifuge	27
Fig. 3.7 Dewater apparatus.....	28
Fig. 3.8 Schematic diagram of core flooding apparatus.....	29
Fig. 3.9 Sectional drawing of core holder	30
Fig. 3.10 Detailed cross sectional view of the core holder	31
Fig. 3.11 Core holder and the core sleeve	31
Fig. 3.12 Data logger system of the core flooding apparatus.....	33
Fig. 4.1 Isothermal emulsion ternary phase diagram	38
Fig. 4.2 Emulsion samples and the compositions in Zone-A of ternary diagram	39

	Page
Fig. 4.3 Emulsion samples and the compositions in Zone-B of ternary diagram	40
Fig. 4.4 Emulsion samples and the compositions in Zone-C of ternary diagram	41
Fig. 4.5 Rheology study results of Zone A micro-emulsions.....	43
Fig. 4.6 Rheology study results of Zone B micro-emulsions.....	44
Fig. 4.7 Rheology study results of Zone C micro-emulsions.....	45
Fig. 4.8 Sample of the optimized micro-emulsion.....	47
Fig. 4.9 Viscosity measurement of the optimized micro-emulsion.....	48
Fig. 4.10 Effect of nanoparticles on the emulsion rheology behavior	49
Fig. 4.11 Viscosity reduction of the crude oil	50
Fig. 4.12 Emulsion pictures under the microscope	51
Fig. 4.13 Picture of the crude oil emulsion	51
Fig. 4.14 Case 1 core flooding experiment oil recovery profile.....	55
Fig. 4.15 Case 1 core flooding effluent collected in the 50 cc plastic tube.....	56
Fig. 4.16 Case 1 core pictures of each core flooding stage.....	57
Fig. 4.17 Case 2 core flooding experiment oil recovery profiles	59
Fig. 4.18 Case 2 core flooding effluent collected in the 50 cc plastic tube.....	60
Fig. 4.19 Case 2 core pictures of core flooding stage	61
Fig. 4.20 Case 3 core flooding experiment oil recovery profiles	63
Fig. 4.21 Case 3 core flooding effluent collected in the 50 cc plastic tube.....	64
Fig. 4.22 Case 3 core pictures of each flooding stage.....	65
Fig. 4.23 Case 4 core flooding experimental oil recovery profiles	67

	Page
Fig. 4.24 Case 4 core flooding effluent collected in the 50 cc plastic tube.....	68
Fig. 4.25 Case 4 core pictures of each flooding stage.....	69
Fig. 4.26 Comparisons of the Berea core flooding experiment results	70
Fig. 4.27 Comparison of the Idaho core flooding experimental results	71
Fig. 4.28 Core flooding oil recovery profile comparison between Case 1 and Case 3	72
Fig. 4.29 Core flooding oil recovery profile comparison between Case 2 and Case 4	73

LIST OF TABLES

	Page
Table 1.1 The oil properties of West Sak fields	4
Table 2.1 Comparison between macro-emulsion and micro-emulsion.	13
Table 3.1 Solvent Kauri-Butanol value table	20
Table 4.1 Crude oil interfacial tension measurement (77°F, 14.7 psi).....	46
Table 4.2 Optimized micro-emulsion interfacial tension measurement	47
Table 4.3 Case 1 core flooding experimental results	54
Table 4.4 Case 2 core flooding experiment results	58
Table 4.5 Case 3 core flooding experiment results	62
Table 4.6 Case 4 core flooding experiment results	66

1. INTRODUCTION

The term, unconventional oil, typically refers to heavy oil (10-20°API), extra heavy oil (<10°API,<10,000cp) and bitumen(<10°API,>10,000cp). With increasing demand for oil of the world, there has been a steady shift of attention to unconventional petroleum resources. Unconventional oil is one of the options. Totally it accounts for almost 70% known and technically accessible fossil fuel resources in the world. In this proposal, we use the term “unconventional oil” to be synonymous with the term “heavy oil”.

Heavy oil resources are located in over 70 countries in the world. A map of Heavy oil locations is presented below in **Fig. 1.1**. There are huge and famous heavy oil resources in Canada, Venezuela, Russia, Alaska and many other countries. Canada and Venezuela, these two countries account for 3.9 trillion barrels of heavy oil reserves.

Due to its very high viscosity and thus extremely low mobility comparing to light oil at reservoir condition, unconventional production methods have been used to extract it. Canada, Venezuela, and the United States maintain the leading position in heavy oil production. In Canada, open-pit mining of the shallow oil sands provides approximately 50% of the nation’s heavy oil production. And cold heavy oil production with sand (CHOPS) and thermal production endows the remainder part. In Venezuela, complex well cold production predominates. In the USA, thermal production by injecting steam is the primary production method. However, there are still several barriers to the growth of the heavy oil production. For example, open-pit mining has a large environmental impact and can only exploit resources near the surface. Also the thermal method due to

the steam generation releases the large amount of CO₂, which leads to the global warming issue. Otherwise, the thermal production needs some strictly unforgiving reservoir geological conditions, in the order of 8 meters, the heat loss to the overburden and underburden formation makes the thermal recovery particularly uneconomical. If the fractures are developed in the reservoir, the problem becomes the heat or steam through the fractures to aquifers formation. Some cases are even more challenging. For instance, the Alaska North Slope heavy oil reservoirs are covered by permafrost which is easy to be destroyed by the steam injection. But there is 30 billion barrels original oil in place in Alaska North Slope area, up to one-fourth of which could be recoverable. The resources there are indispensable to fill the fossil fuels gap for the United States energy demands in the next decade even with aggressive development and deployment of new renewable and nuclear technologies.

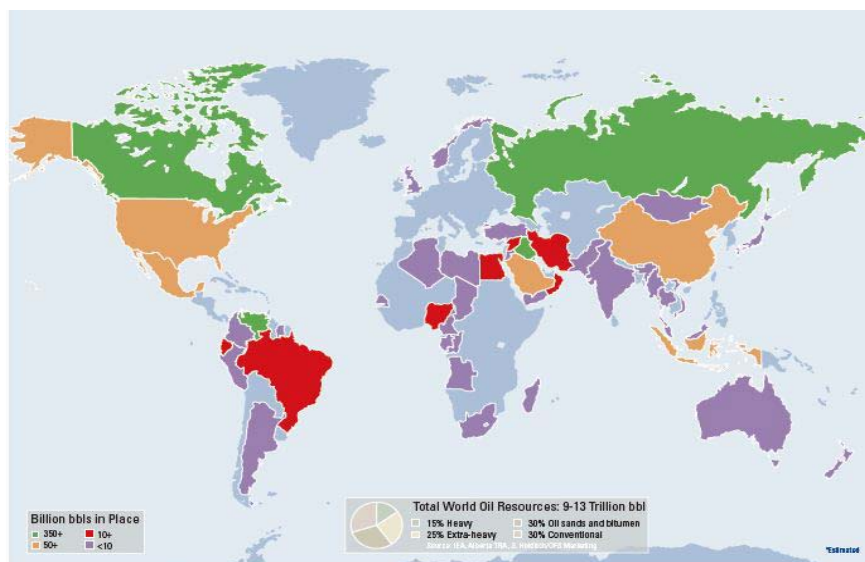


Fig. 1.1 Distribution of worldwide heavy oil resources (Thomas 2007)

1.1 Overview of Alaska North Slope Heavy Oil

The Alaska North Slope is famous for its secondary large heavy oil reserves in United States, primarily in two remote area, the West Sak and Ugnu sands. **Fig. 1.2** shows the ANS area below.



Fig. 1.2 Map of ANS area and distribution of oil extraction activities (Thomas 2007)

In the research, I use oil samples obtained from West Sak field. **Table 1.1** lists the oil properties in ANS area and Ugnu.

Table 1.1 The oil properties of West Sak fields

	West Sak Field	Ugnu Field
Oil Gravity	12 – 23 °API	7.1 – 11.5 °API
Temperature	45 – 100 °F	45 – 65 °F
Porosity	15 – 40 %	25 – 37 %
Viscosity	30 – 3000 cp	60000 – 10000000 cp
Permeability	150 – 500 md	100 – 3000 md
Oil Saturation	60 – 70 %	66 – 72 %
Lithology	Sandstone	Sandstone
Net Pay Thickness	90 ft	75 – 100 ft
Oil in place	13-18 billion barrels of oil	7-10 billion barrels of oil

1.2 Main Challenges in ANS Heavy Oil Reservoirs

Based on the published information, the main challenges in developing heavy oil reservoir in Alaska North Slope area include:

- Technical challenge to applying thermal recovery methods because the reservoir is proximity to the permafrost
- Sand control and disposal problems in remote arctic environment due to unconsolidated sand
- High asphaltene content
- Low in-situ permeability.

1.3 Chemical EOR in Developing Heavy Oil Reservoir

Fortunately, chemical enhanced oil recovery (EOR) is a possible EOR method for development of the ANS heavy oil reservoirs. A chemical EOR method may utilize the

facilities built in Alaska oil fields and would not destroy the permafrost over the reservoir and would not affect the formation as thermal EOR would. However, there is not sensitive to the geological condition like thermal production. However, there is no on-going commercial industry project using the chemical EOR in Alaska heavy oil reservoirs. And there are only three or four small chemical EOR projects in conventional oil reservoirs in the United States. Only a few exploratory researches in heavy oil chemical EOR area published in recently years. My research is also an exploratory research in this area.

Compared with the conventional chemical EOR methods used in conventional oil reservoir, some new ideas have been developed in the research stemming from the differences between light oil and heavy oil properties. In my research, heavy oil viscosity reduction is the key factor in the enhanced oil recovery process and heavy oil in situ emulsification is another critical factor.

This research presents an experimental evaluation of the potential application of solvent based emulsion to recover heavy oil from the thin, cold, permafrost over or other kind of steam-non-suitable reservoirs. The solvent based emulsion flooding can provide the high displacement efficiency like miscible solvent flooding and better sweep efficiency like polymer flooding.

The main mechanisms involved in improved recovery of heavy oil by solvent based emulsion flooding include:

1. *Mobility control*. The mobility of a solvent-in-water(S/W) emulsion is generally much lower than the mobility of solvent or water alone. Also the addition of

nanoparticles could thicken the solvent-in-water(S/W) emulsion to the desirable mobility. Therefore this emulsion flooding will be less prone to viscous fingering and should lead to improved sweep efficiency.(Healy et al. 1975)

2. *Oil viscosity reduction.* Pure miscible solvent injection could make huge solvent mass transfers into heavy oil and then reduce viscosity of the heavy oil impressively but not economically due to the high cost of solvent with respect to the market value of the heavy oil recovered. But, the injection of the solvent-in-water(S/W) emulsion with the O/W surfactant could make crude oil in water emulsion. And since the water molecules surround crude oil molecules and the solvent dissolve in viscous oil, the oil-in-water emulsions has low viscosity comparing with the original crude oil. (Bryan et al. 2008)
3. *In situ emulsification of heavy oil.* The solvent based emulsion contains the organic solvent, surfactant and the nanoparticles. The crude oil could emulsify and form low viscosity, oil-in-water emulsions immediately with the assistant of solvent, surfactant and nanoparticles.(Bryan et al. 2007; Zhang et al. 2009)

1.4 Objective

Overall project objective is to conduct a program of Chemical Enhanced Oil Recovery research to develop technology to exploit and market the heavy oil resource found in the Alaska North Slope area. This thesis focuses on the recovery of 300 to 3000 cp heavy oil in the West Sak field.

Specific objectives included:

- I. Investigate the fundamental solvent based emulsion flooding mechanisms in heavy oil reservoir
- II. Evaluate the solvent-based emulsion and heavy oil emulsion property (IFT, Phase behavior and Rheology, etc) to find the technical and economical feasible emulsion to develop the reservoir.
- III. Study on core flooding to analyze the EOR recovery effect.
- IV. Collect relevant data needed to simulate in-situ recovery processes for the recovery of North Slope heavy oils, especially West Sak.

2. ENHANCED OIL RECOVERY-AN OVERVIEW

Five trillion barrels of heavy oil worldwide will remain in the reservoir after primary and secondary recovery methods have been utilized. Most of this heavy oil may probably be recovered by enhanced oil recovery (EOR) methods. The EOR method chosen for a particular reservoir depends on geological, technological as well as economical factors. But only a few EOR methods have been carried out in the field successfully, such as steam injection in heavy oil reservoir and miscible carbon dioxide for light oil reservoirs. The industry currently applies the thermal method to develop the heavy oil reservoir such like cyclic steam injection, steam-flooding, steam assisted gravity drainage (SAGD) and in situ combustion. Many chemical EOR projects were operated in the 1980's worldwide, some of which were successful, but most failed. The chemical EOR operations are not active currently except in China. However the industry gained valuable experiences and a better understanding of chemical EOR since the research has not been interrupted in last 30 years. And because of the environmental and geological issues related to thermal method and the vast heavy oil reserves, the industry has recently embarked on investigation on the feasibility of chemical EOR application in heavy oil reservoirs. (Mai et al. 2009)

EOR refers to the processes that increase oil recovery by reduction of the residual oil saturation after primary and secondary production. And the objectives of an EOR process depend on the oil type. **Fig. 2.1** shows the different EOR targets for typical light oil, heavy oil and bitumen. Heavy oil and bitumen have very poor response to primary

and secondary recovery methods and it is necessary to apply EOR technology at the beginning of the reservoir development.

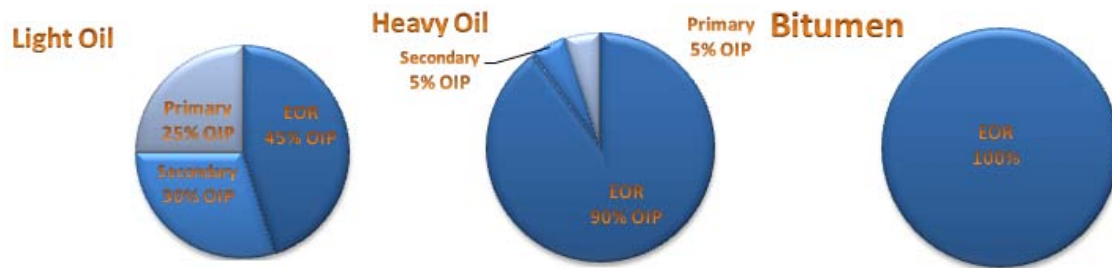


Fig. 2.1 EOR target for different hydrocarbons (Thomas 2007)

Fig. 2.2 shows the classification of the popular EOR methods. In this thesis, we investigate the mechanism of a novel emulsion flooding to enhance heavy oil recovery.

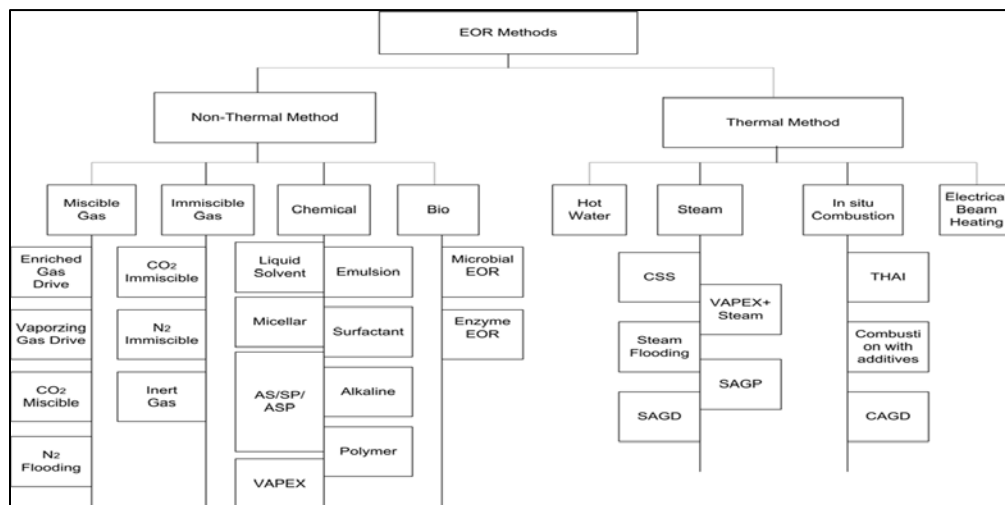


Fig. 2.2 The classification of enhanced oil recovery method (Thomas 2007)

2.1 EOR Mechanism

Generally, the oil recovery factor may be viewed as consisting of two parts, displacement efficiency (E_D) and sweep efficiency (E_S). Displacement efficiency is controlled by capillary number (N_c) and mobility ratio (M) dominates the sweep efficiency. Capillary number is defined as $N_c = v\mu/\sigma$, where v is the Darcy velocity and μ is the viscosity of the displacing fluid, σ is the interfacial tension.

The capillary forces are responsible for oil droplet trapped in the porous medium, and the entrapped oil could be mobilized only by exceeding the capillary force. Capillary number is a significant parameter to evaluate the interaction between the viscous force and capillary forces. Both of them directly affect the residual oil saturation.

The best and most effective way to increase the capillary number is to reduce the interfacial tension by using a feasible surfactant or by reducing the oil viscosity through injection of heat. Based on published results, a 50% reduction in residual oil saturation (ROS) needs an increment of three orders of magnitude of capillary number (**Fig. 2.3**).

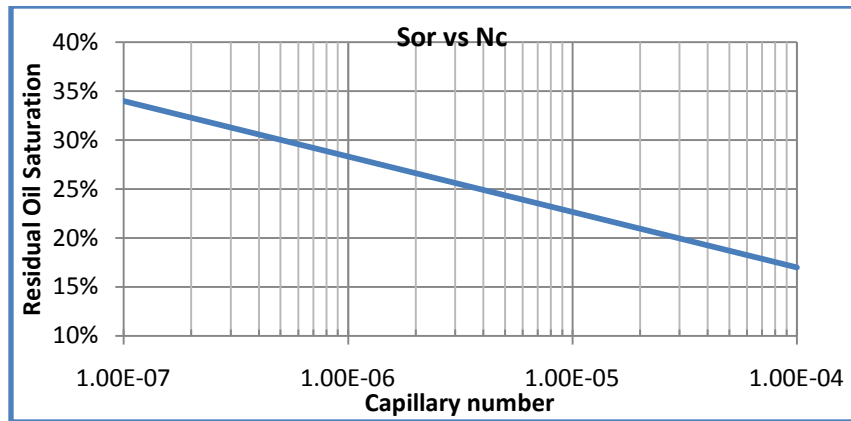


Fig. 2.3 Relationship between ROS and capillary number(Thomas 2007)

A miscible flooding could be understood as a process when the interfacial tension becomes zero since the displacing phase. In this case, the capillary number is infinity and the residual oil saturation is zero.

Mobility ratio is the dominant factor affecting sweep efficiency. Mobility of a phase p is defined as the porous material permeability of the phase divided by the viscosity, i.e. k_p/μ_p . Mobility ratio, M , is defined as mobility of the displacing phase divided by the mobility of the displaced phase. The case, $M > 1$, is considered unfavorable and unstable, because the displacing fluid (e.g. water) is more readily to flow other than the displaced fluid (e.g. oil), and it can lead serious viscous fingerings or channeling of the displacing fluid. As a result, some of the residual oil is bypassed. In contrast, the sweep and displacement efficiencies are increased when $M \leq 1$, and is denoted as a “favorable” mobility ratio. **Fig. 2.4** shows the comparisons between the two cases of M .

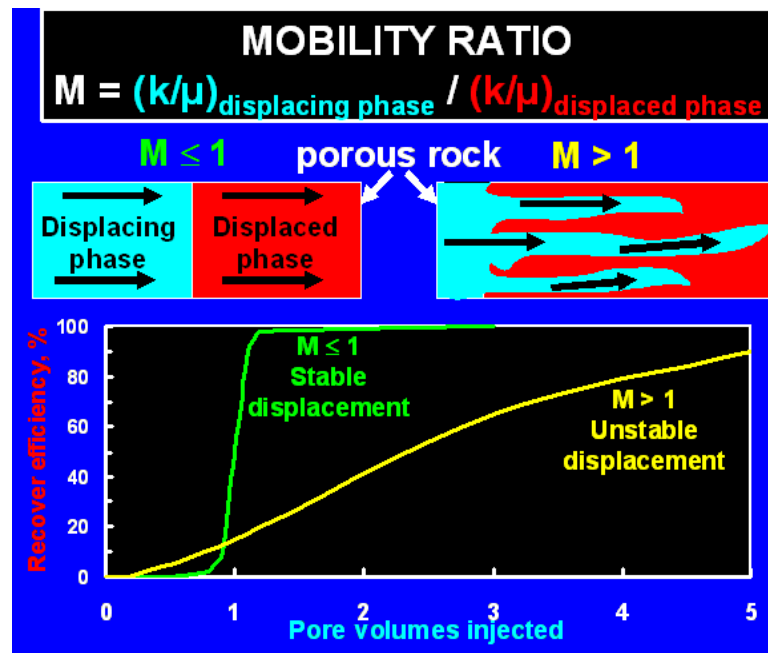


Fig. 2.4 Comparisons between the two cases: $M > 1$ and $M \leq 1$ (Seright 2006)

2.2 Micro-emulsion and Macro-emulsion

For a three components emulsion system, the micro-emulsion is the counterpart of the macro-emulsion since they both belong to the system but with different characteristics. The study of micro-emulsion began in the late 1960s, encouraged by the long emulsion stability and ultra-low interfacial tension of the micro-emulsion. The petroleum industry started research into the tertiary micro-emulsion recovery method EOR research in the 1970s. (Healy, et al. 1975)

Table 2.1 shows a comparison of the main properties between macro-emulsion and micro-emulsion. The size of a micro-emulsion droplet is of the order of nanometers and

the micro-emulsion is clearly transparent and thermodynamically stable. In contrast, the macro-emulsion will separate into two phase again after a specific time.

Table 2.1 Comparison between macro-emulsion and micro-emulsion

	Macro-emulsion	Micro-emulsion
Stability	Kinetically	Thermodynamically
Transparent	No, milky white	Yes or low turbidity
Size	Mainly 0.1-10 mm	10-200 nm
Formation	No	Spontaneous
Type	o/w, w/o, w/o/w, o/w/o	o/w, w/o, cylinder

Healy et al. (1974) constructed the ternary phase diagrams for three specific micro-emulsion systems to show the effects of the salinity and co-surfactant on phase behavior, viscosity, and interfacial tension.

Healy et al. (1975) conducted the laboratory micro-emulsion core flooding study. He proposed that the micro-emulsion flooding involved both miscible and immiscible aspects which are affected by injection rate. Residual oil saturation decreases with increased surfactant concentration.

Willhite et al. (1980) performed the laboratory studies of micro-emulsion oil recovery mechanisms by investigating the phase behavior and conducting core flooding experiments. They reported that a milky white macro-emulsion effluent was observed and they suggested the single pseudo ternary phase diagram may be not enough due to the variation of the concentration of the surfactant to the oil phase ratio.

Bennett et al. (1981) examined the rheological properties of the micro-emulsion and reported the Newtonian and Non-Newtonian behavior.

Bouabboune et al.(2006) made the comparisons between micro-emulsion flooding and surfactant flooding efficiency in a light oil reservoir. They pointed out that the micro-emulsion flooding process is the unique and effective method for the high water containing or depleted reservoir. They optimized the surfactant concentration and micro-emulsion viscosity for the flooding purposes. They concluded that micro-emulsion flooding is more efficient than the surfactant flooding.

2.3 Chemical EOR in Heavy Oil Reservoir

In heavy oil development case, after the primary and secondary production, the residual oil is largely bypassed due to viscous finger caused by the adverse mobility ratio between oil and water. The bypassed oil is not like the residual oil in light oil reservoir is discontinuous ganglia. Consequently, numerous chemical EOR researches are conducted to improve oil recovery after water flooding in heavy oil reservoir.

Generally, the heavy oil chemical EOR technology can be applied to the heavy oil reservoir containing oil of 10° to 20° API gravity and viscosities below 15,000 centipoises.

In this research, solvent, surfactant and nanoparticles are used at low concentration levels in water and help reduce viscosity by forming a water-external crude oil emulsion. It is an economical and environmental friendly alternative to other heavy oil recovery techniques such as steam flooding. Also a wide range of temperatures and salinity resistance can be tolerated by this emulsion system.

Binder *et al.* (1965) raised the idea to inject an oil-in water emulsion to improve the heavy oil recovery in his patent. They recognized the necessity to increase the displacing fluid viscosity to tune the mobility ratio during the viscous oil reservoir water flooding. They mentioned that the oil-in-water emulsion might make up the whole driving fluid body or a portion of the driving fluid. The core flooding results indicated that 78% of the oil in place was recovered at the breakthrough and 83% recovery factor was reached by injecting one pore volume emulsion. And the produced emulsion was very similar in characteristics to the emulsion injected.

McAuliffe *et al.* (1973) reported the first oil field application in emulsion flooding. The field trial was in Section 5K of the Midway Sunset field, California. The emulsion with average droplet diameter in 3 microns and viscosity in 200 cp were pumped into the well. In the 2-year period, three emulsion injection wells showed lower water cut and increased oil recovery and water tracer studies showed that sweep efficiency was improved. In all 33,000 bbl of crude oil emulsion (3 percent of PV) was injected, while 55,000 bbl of additional oil had been produced.

Van der Knaap *et al.* (1970) mentioned the simultaneous injection of solvent and water into high-viscosity crude oil reservoir, and the solvent only occupied a small amount in the injected fluid. Also the solvent could be re-injected after it was recovered from the produced fluid. The simultaneous injection could form unstable solvent in water emulsion which could overcome the viscous finger tendency of the solvent alone.

Bousaid (1978) proposed a surfactant stabilized solvent in water emulsion injection to improve heavy oil recovery method. The surfactant concentration may vary during the

injection process and different hydrocarbon as solvent could be used in making the emulsion.

Sarma et al (1995) summarized the mechanism of the solvent in water emulsion flooding including mobility control, viscosity reduction by solvent dissolution, oil mobilization by in situ emulsification and phase interfacial tension reduction. The viscosity reduction improved but mobility control worsened with the surfactant concentration decreasing. The economical evaluation of solvent in water emulsion flooding shows that the continuous injection is not economical.

Bryan et al (2007) investigated the potential application of the alkali-surfactant flooding in heavy oil reservoir. The in situ emulsification is the main mechanism for this process due to both alkaline and surfactant could lower the interfacial tension between water and oil phase. The experiment results suggest the water-wet rock and oil in water emulsion are preferred because the low viscosity character of the O/W emulsions could facilitate the production.

Flaaten et al (2008) and Zhang et al (2009) discussed the potential application of the nanoparticles stabilized emulsion system in petroleum industry. The toluene in water emulsions are generated with assistant of a bit of nanoparticles. The study of the emulsion stability and phase behavior are reported and the emulsion's piston-like front flooding is observed.

In summary, previous research provide a general but not very clear direction in application of solvent in water or oil in water emulsion flooding in the development of

heavy oil reservoir. In this thesis, I would like to continue an exploratory research in this area and propose a solvent-emulsion meth.

3. EXPERIMENTAL SET-UP AND PROCEDURES

The experimental study can be generally divided into two parts:

(1) Bench tests of the properties of solvent based emulsion and the crude oil emulsion.

(2) Core flooding experiments to investigate the effect of the various injection on oil recovery factor.

3.1 Experimental Materials

3.1.1 Sandstone Core

Two different sandstone cores were used in the core flooding experiment. The permeability of Buff Berea core is 200 mD and Idaho sandstone core is 800 mD. All the cores are in cylinder shape with 12 in long and 1 inch in diameter.

3.1.2 Nitrogen

Nitrogen was used to maintain the back pressure of the production system. It was stored in cylinders with an initial pressure of 2500 psi.

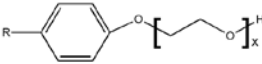
3.1.3 Crude Oil

The crude oil comes from the West Sak in Alaska North Slope area provided by British Petroleum, which has an oil gravity of 16.35°API or 0.9513 g/cm³ after dewatering in the lab.

3.1.4 Brine Solution

1wt% sodium chloride was added to the de-ionized water to make the 10000ppm NaCl brine solution. The brine solution was used to saturate and flood the core and make the solvent base emulsion.

3.1.5 Surfactant

The nonionic surfactant, Triton X-100 (Octyphenol Ethoxylate) was used to make emulsion. The surfactant formula is . The HLB of the surfactant is 13.5, so it intends to help generate oil in water emulsion. The viscosity is 240cp at 77°F.

3.1.6 Nanoparticles

Nanoparticle- CAB-O-SIL® TS-530 is used to stabilize the emulsion with the surfactant. It could thicken the solvent based emulsion and provide excellent sag resistance flow character which means less absorption by the rock. Also due to the high surface area, it could help form emulsion with no or less surfactant needed.

3.1.7 Solvent

The solvent, xylene, plays as the oil phase part in the solvent based emulsion system. According to the Kauri-butanol value (“Kb value”) table which is an international standardized measure of solvent power for a hydrocarbon solvent, xylene is one of the most powerful solvent. (See **Table 3.1**)

Table 3.1 Solvent Kauri-Butanol value table

	kauri-butanol value
Iso-hexane	27.5
Hexane	30
n-Pentane	33.8
Iso-heptane	35
Heptane	35.5
isooctane	38
benzene	107
toluene	106
xylene	103

3.2 Emulsion Bench Test Set-up and Procedure

The bench test includes emulsion phase behavior scan, interfacial tension measurement and rheology model study. These three properties of the emulsion are primary determinants of the potential success of core flooding. The study of phase behavior of emulsion is a matter of emulsion types, stability, phase inversion, salinity resistance and preparation method. And the purposes of the solvent based emulsion phase behavior are to find the feasible and economical emulsion composition and that is the crucial factor for the success of the emulsion flooding. Interfacial tension is another important evaluation criterion of the efficiency of the emulsion system. The low interfacial tension is preferred. Rheology model study could help us to better understand the enhanced oil recovery mechanism of the emulsion flooding.

3.2.1 The Phase Behavior Scan Set-up and Procedure

A large number of glass tubes are used to investigate the solvent based emulsion phase behavior in the laboratory condition (ambient temperature is 25 °C). Burettes with

fine gradations and a stopcock at the bottom are used for accurate surfactant, solvent and brine volume measurement. See **Fig.3.1**.



Fig. 3.1 The emulsion phase behavior experiments in the hood

The procedure to make solvent emulsion is summarized as follows:

1. Prepare the glass tubes and fill the two different burettes with Xylene and TX-100
2. Make 10000 ppm NaCl brine by using de-ionized water and reagent grade NaCl.
3. Mix the solvent, TX-100 and brine with different concentration in the glass tubes and agitate them in the ultrasound bathtub. The critical emulsion compositions which could separate the diagram into micro-emulsion and macro-emulsion region were examined by adding five drops (250 μ l) water into one verified micro-emulsion one time and waiting for at least one hour to check the possible changes until the separation phenomena or macro-emulsion performed. Totally, about hundreds of the experiments have been done.
4. Observe the emulsion for a minimum of 12 hours to sort the emulsion type based on the emulsion stability, emulsion transparency, emulsion droplet size and emulsion formation.

3.2.2 Emulsion Droplet Size Measurements

The emulsion droplet size measurement equipment consists of a ProgRes CT 5 digital camera attached to one MEIJI 9920 polarizing microscope. The microscope-camera system is connected to a computer with imaging software. See **Fig.3.2**.



Fig. 3.2 The microscope and the digital camera

3.2.3 Surface Tension Measurements

There are two surface tension meter equipments: Sigma 703 for surface tension measurement and Kruss DSA30 IL4200 for interfacial tension measurement. See **Fig.3.3**.

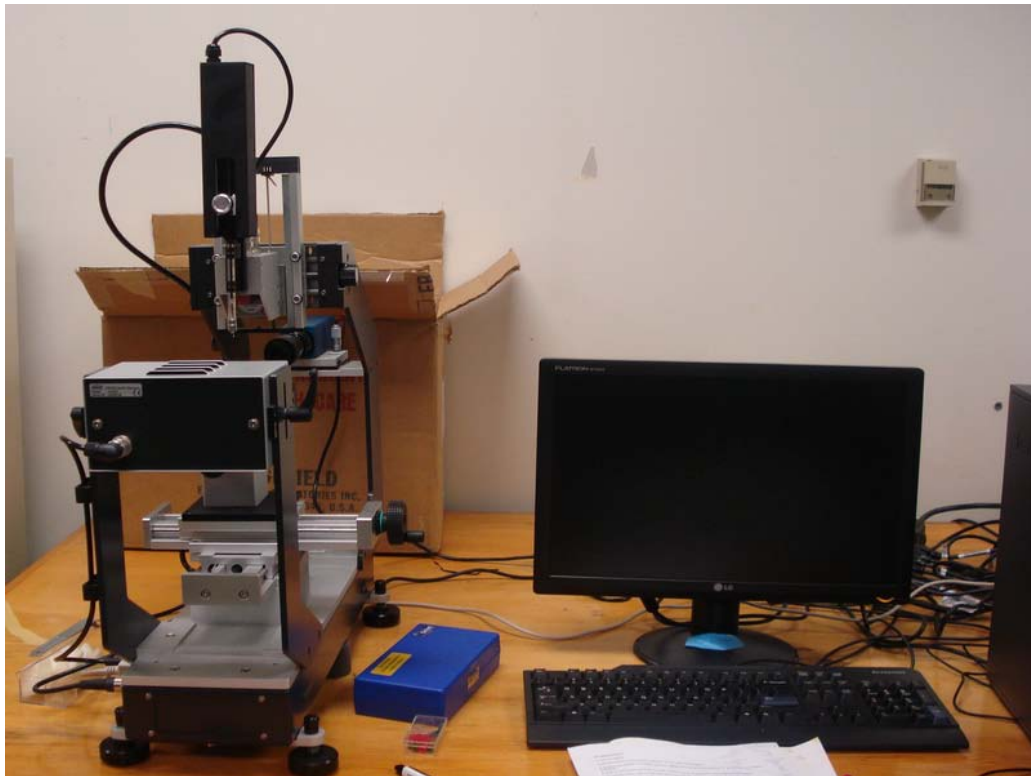


Fig. 3.3 Kruss DSA30 IL4200 interfacial tension meter

3.2.4 Viscosity Measurements

The Brookfield DV-III Ultra rheometer with the temperature control equipment are used to study the emulsion rheology model and measure the viscosity of oil sample and emulsion sample. See **Fig.3.4**.



Fig. 3.4 DV-III Ultra rheometer and the temperature control equipment

3.2.5 Other Apparatus

The Ultrasound tub assists to make solvent based emulsion in shorter time by generating a cyclic sound pressure with a high frequency. See **Fig.3.5**.

The electric blender with high shear rate range could help to make the crude oil emulsion.

The centrifuge is used to separate the core flooding effluents. See **Fig. 3.6**.



Fig. 3.5 Ultrasound tub (left) and high speed range blender



Fig. 3.6 Centrifuge

3.3 Oil Dewatering Apparatus

The original oil sample needs dewatering to remove residual water before the oil can be used in the bench test and core flooding experiments. The principle of dewatering is to utilize the boiling point difference under the vacuum pressure condition. The water's boiling point is much lower than those of the heavy oil fractions, so the water can evaporate from the oil. The light oil fractions are condensed with the aid of liquid nitrogen placed in tubes. See **Fig. 3.7**.



Fig. 3.7 Dewater apparatus

3.4 Core Flooding Apparatus

Core flooding experiments were performed as validation for the promising solvent based emulsions which were identified during the phase behavior scan experiments. The core flooding apparatus consists of four main parts: core holder and confinement system, injection system, production system and data log system. The schematic diagram of the system is shown in **Fig.3.8**.

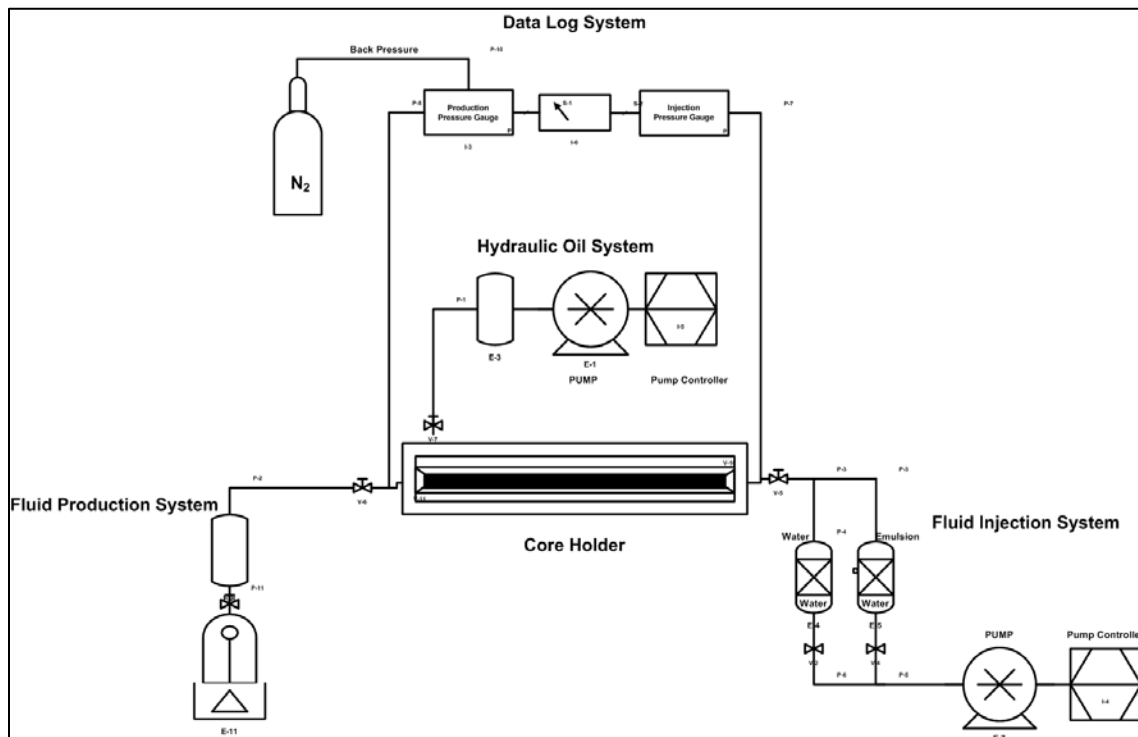


Fig. 3.8 Schematic diagram of core flooding apparatus

3.4.1 Core Holder

The core holder in **Fig.3.9**, **Fig. 3.10**, and **Fig. 3.11** is designed for reservoir condition core flooding experiment. It is capable of holding cores up to 1 ft. in length and 1 in. in diameter. The maximum pressure rating of the core flood cell is 7000psi. The core holder consists of detachable end pieces with plungers on both ends. One end has a fixed plunger and the other plunger can be moved by rotating a screw to check the core is perfectly in contact with the distributor. In the experiment, the core with 1 in diameter and 12 in length is perfectly fit the core holder.

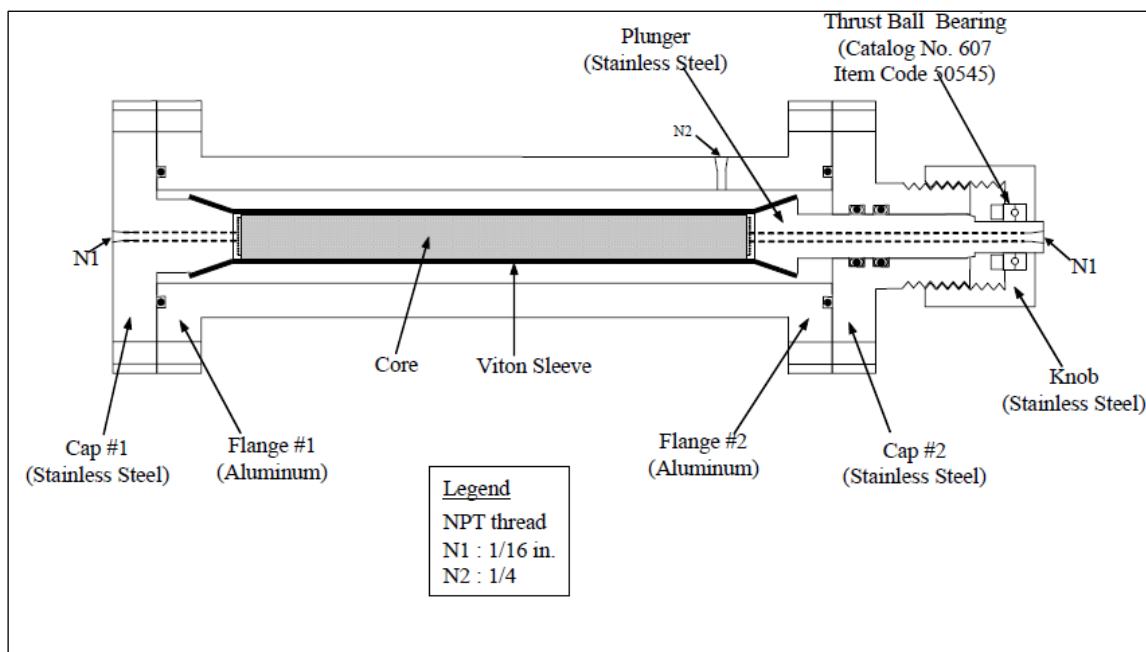


Fig. 3.9 Sectional drawing of core holder

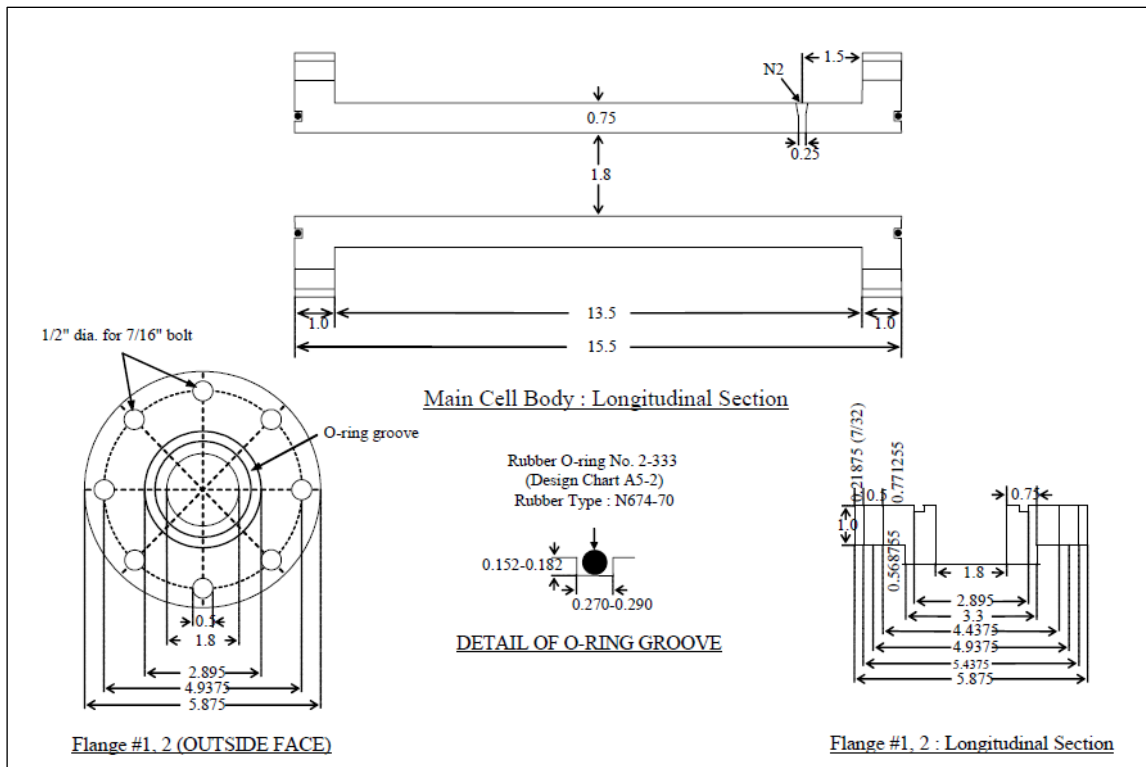


Fig. 3.10 Detailed cross sectional view of the core holder



Fig. 3.11 Core holder and the core sleeve

3.4.2 Injection System

The fluid injection system consists of one syringe pump and three sets of 500ml accumulators for brine, emulsion and oil separately (the accumulator for oil not in the core flooding scheme). The liquid was delivered by a Teledyne ISCO 500D syringe pump using stainless steel tubing. The pump with a nominal cylinder capacity of 507 ml, consists of a programmable pump controller. The syringe pump 500D is ideal for a wide range of chemical feed applications requiring flow rates from 0.01 ml/min to 200 ml/min at pressures up to 3,750 psi. The water is injected from the pump below the piston in the accumulator. In the experiment, the flow rate is set as 0.5ml/min in a single fill.

3.4.3 Production System

The fluid production system consists of one separator (A 150 cc stainless steel, with a high pressure) and one centrifuge (**Fig.3.6**) to help separate the core flooding effluent. The separator outlet pressure maintained at a constant pressure of 100 psig by connecting to the nitrogen cylinder. And the produced effluents were collected at the bottom of the separator in the plastic tubes.

3.4.4 Data Logger System

Two pressure transducers at the inlet and outlet were used to measure the injection pressure and production pressure. The data are transferred to the data logger system and recorded in one personal computer. See **Fig.3.12**



Fig. 3.12 Data logger system of the core flooding apparatus

3.5 Core Flooding Experiment Procedure

Prior to beginning an experiment, all core flooding apparatus were thoroughly cleaned to exclude any presence of oil traces and any particles. The pump, pressure transducers and gauges and data logger were calibrated and checked. The experiments were conducted in the ambient temperature which is only a little lower than the reservoir temperature.

The core flooding follows the standard procedure as follows:

1. Place the core in the aluminum core holder and apply confinement pressure of 300-500 psi above the injection pressure.
2. Evacuate the core holder in the oven under temperature (60 °C) overnight. This is established by connecting the core holder outlet to a vacuum pump while the core holder is placed in the oven.
3. Weigh the dry core.
4. Inject 2-3 PV of the prepared brine to make steady state and hence completed water saturation. The amount of water entering the core should be recorded. Use this step to apply Darcy's law and measure the permeability of water phase.
5. Weigh the 100% brine saturated core.
6. Calculate the core's porosity using the material balance calculations by using the weight of dry and saturate core and brine density.
7. Saturate the core with oil to bring the core to connate water. It is achieved by injecting 2-3 PV of oil at 0.05cc/min until a steady state flow rate is reached and no more water is produced.

8. Weigh the oil saturated core.
9. Calculate oil saturation by material balance calculations.
10. Water floods the core until only water is produced.
11. Weigh the core then calculate the recovery factor after the water flooding.
12. Emulsion floods the core with the reasonable PV injection.
13. Weigh the core and weigh the effluent of emulsion flooding then calculate the recovery factor after the emulsion flooding.

4. EXPERIMENTAL RESULTS AND DISCUSSION

Hundreds of the solvent emulsion bench test experiments were performed, and the phase behavior of the solvent emulsion was observed. Based on these observations, a ternary phase behavior diagram was drawn. The viscosity and interfacial tension of 60 selected emulsions were tested in order to screen the emulsion composition for core flooding. Finally, four successful core flooding experiments were performed. A detailed discussion of the above experiments is given below.

4.1 Experimental Conditions

An overview of the experimental conditions is presented in this section.

4.1.1 Bench Test Experimental Conditions

The solvent emulsion phase behavior experiments and interfacial tension measurements were carried out at ambient pressure and temperature. The viscosity of the emulsion and crude oil were measured at 77°F since the West Sak oil reservoir temperature is between 45°F and 100°F due to the overlying permafrost.

4.1.2 Core Flooding Experiment Conditions

The core flooding experiments are performed in the oven which was set at a temperature of 77°F. The core confining pressure was provided by a hydraulic oil injection system described in the Section 3. The water and solvent base emulsion injection rate was set at 0.5 ml/min.

4.2 Bench Test Experiments

4.2.1 Emulsion Phase Behavior Experiments

Surfactants can form emulsion since they contain both hydrophobic groups and hydrophilic groups. Therefore, they can lower the interfacial tension between oil and water by adsorbing at the liquid-liquid interface. The organic solvent, like xylene, is the perfect candidate to dissolve and mobilize heavy oil in the reservoir. From the economical and technical consideration, the emulsion made by surfactant, solvent and brine appears to be logically sound as it the advantages of the solvent and surfactant.

The micro-emulsion is the desired emulsion type in this research since it provides lower interfacial tension and impressive stability which would be advantageous for storage and transportation purposes. In order to characterize the micro-emulsion, it is first necessary to construct the ternary phase diagram. The relative amounts of the three emulsion components can be represented in the diagram, where their corresponding volume fraction is 100%. Each point in the diagram represents a possible composition of the emulsion and the most direct way to investigate the emulsion phase behavior is the distinguished property of the micro-emulsion- transparency and thermal-dynamical stability.

The emulsion ternary phase diagram is shown in **Fig.4.1**. The spots in the diagram represent the critical composition of the solvent based emulsion which was examined by the method described in the Section 3. In the upper region, the solvent based micro-emulsions are achieved and the macro-emulsions appear in the lower region of the ternary phase diagram. The surfactant critical concentration of the micro-emulsion does

not surpass the 10wt% of the total mass. This index is dominated by the natural property of the surfactant. The data table listing is presented in the appendix.

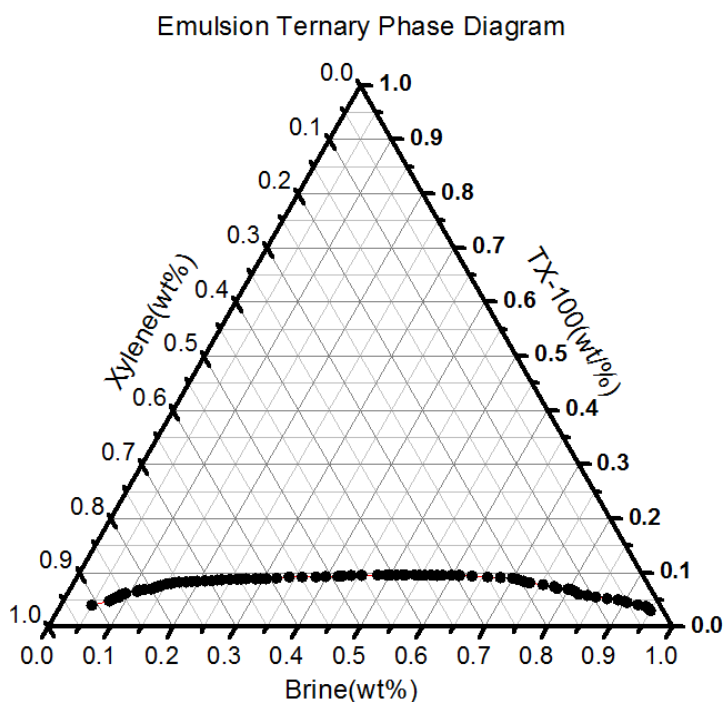


Fig. 4.1 Isothermal emulsion ternary phase diagram

Based on the observations and rheology studies of the emulsion, the micro-emulsion region can be sub-divided into three parts, namely, zone-A, zone-B and zone-C. **Fig.4.2**, **Fig.4.3** and **Fig.4.4** show some emulsion samples (including the macro-emulsion) and their compositions in the above three zones. And the detailed rheology study will be discussed in the next section.

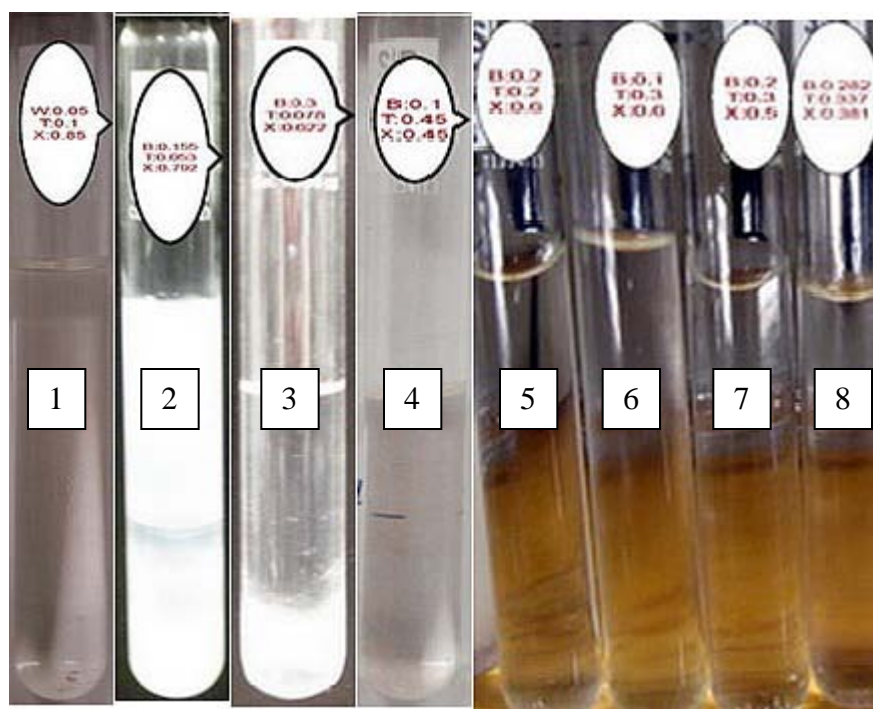
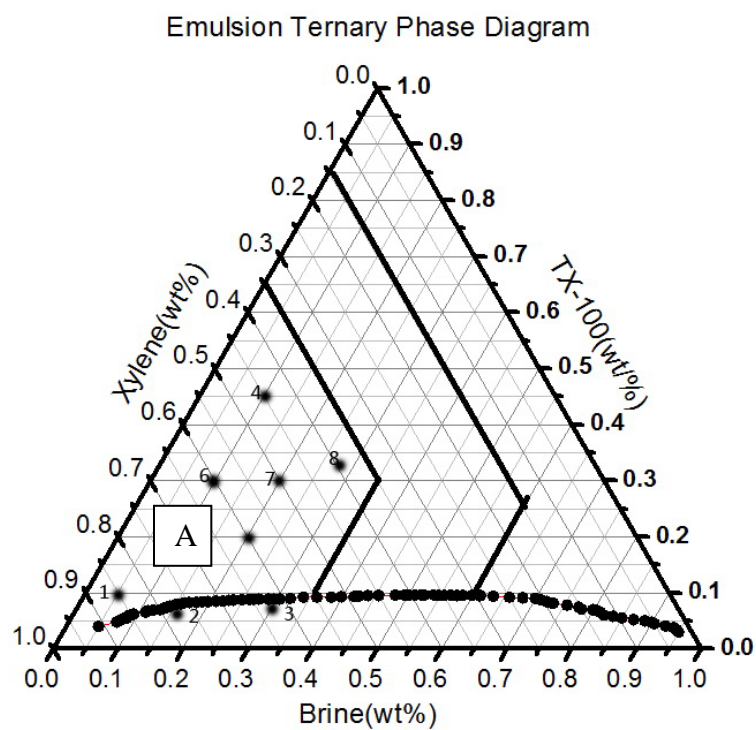


Fig. 4.2 Emulsion samples and the compositions in Zone-A of ternary diagram

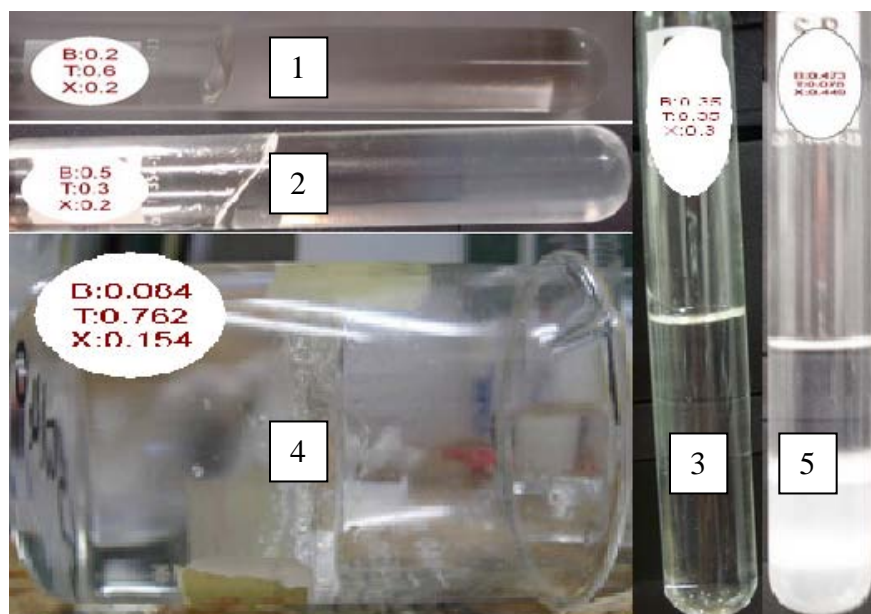
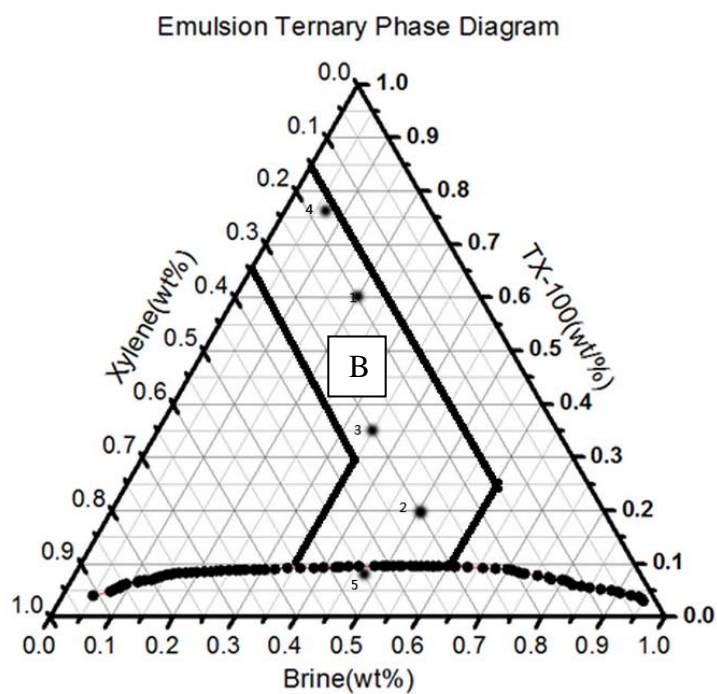


Fig. 4.3 Emulsion samples and the compositions in Zone-B of ternary diagram

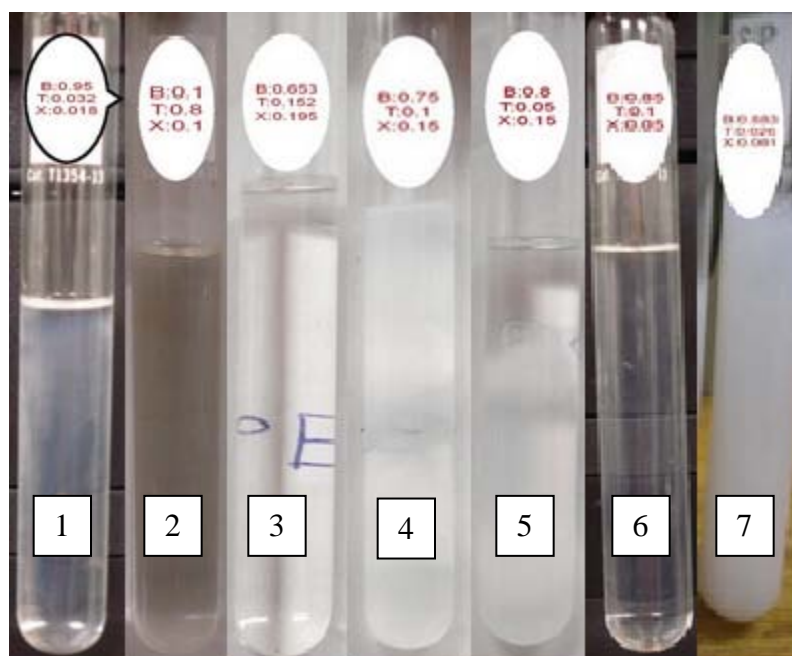
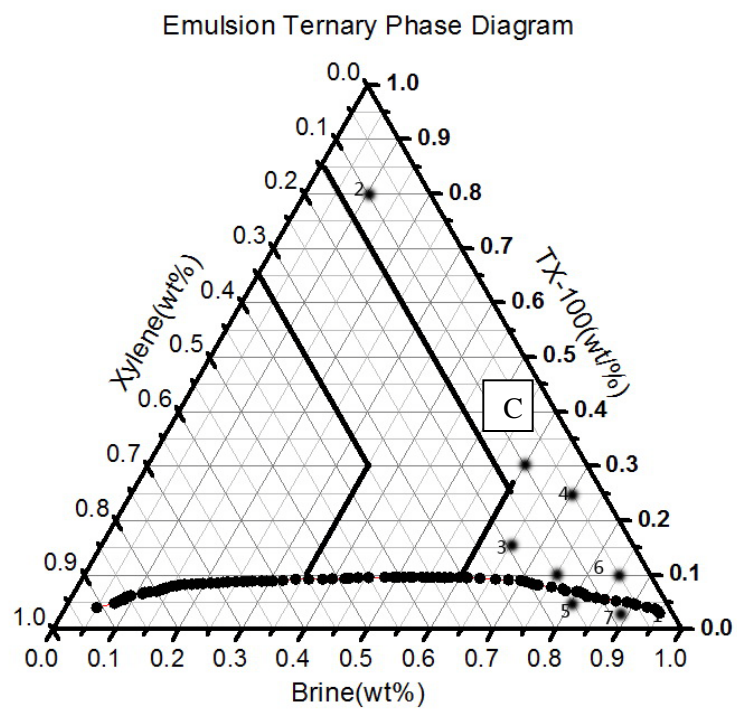


Fig. 4.4 Emulsion samples and the compositions in Zone-C of ternary diagram

4.2.2 Emulsion Rheology Study Experiments

The rheological measurement of the emulsion is a valuable tool for understanding the properties of emulsion during the storage and injection process. And also the emulsion rheology is related to the emulsion stability.

The solvent based emulsion shows the shear-thinning properties which mean that the viscosity decreases with increasing shear rate. And in general, zone C shows a moderate shear thinning behavior and zone A and zone B are more like Newtonian fluid.

And the micro-emulsion region is divided into three zones based on the difference of the three micro-emulsion rheological behavior.

Fig.4.5, Fig.4.6, Fig.4.7 show plots of micro-emulsion viscosity against shear-rate in the logarithmic coordinates. Straight line fits to the data may be constructed. The results indicate the rheology may be described by the following a power-law expression.

$$\mu = K \left(\frac{\partial u}{\partial y} \right)^{n-1}$$

Where K is the flow consistency index (SI units Pa•s), $\partial u/\partial y$ is the shear rate (SI unit s^{-1}), and n is the flow behavior index (dimensionless) and for a shear-thinning fluid $n < 1$.

Zone-A in **Fig 4.5** shows that the apparent viscosity is lower compared with that in the other two zones and indicates a weak shear-thinning property. Because the micro-emulsion's oil phase-xylene-plays a critical role in this region, it makes the emulsion apparent viscosity relatively low.

Zone-B in **Fig.4.6** exhibits the formation of the gel micro-emulsion. Some of the micro-emulsions even cannot flow after the emulsion formation in the ambient

environment. Apparent viscosity of the micro-emulsions can be very high and also they show a moderate shear-thinning rheological behavior in the experiments.

Zone-C micro-emulsion in **Fig.4.7** shows an obvious shear thinning behavior.

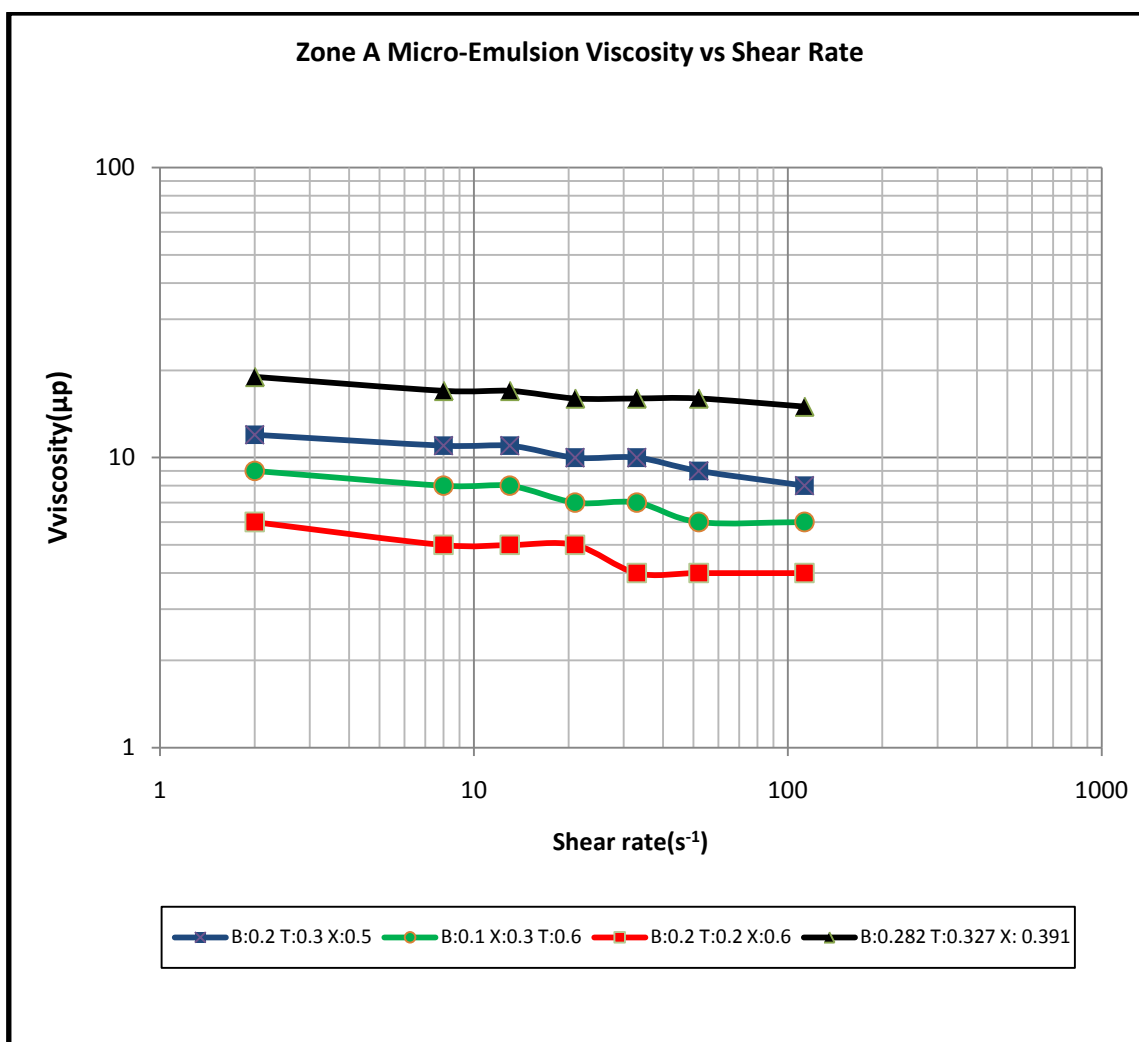


Fig. 4.5 Rheology study results of Zone A micro-emulsions

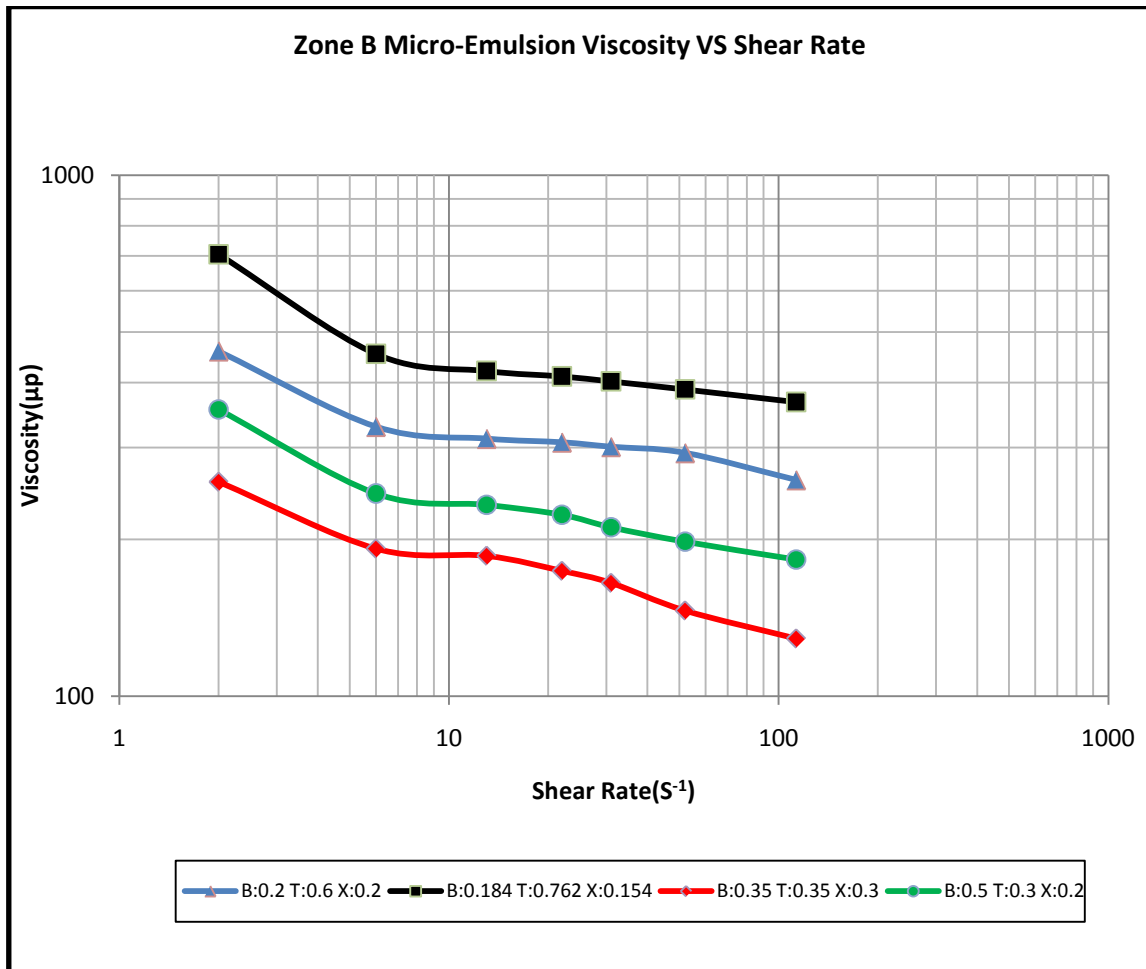


Fig. 4.6 Rheology study results of Zone B micro-emulsions

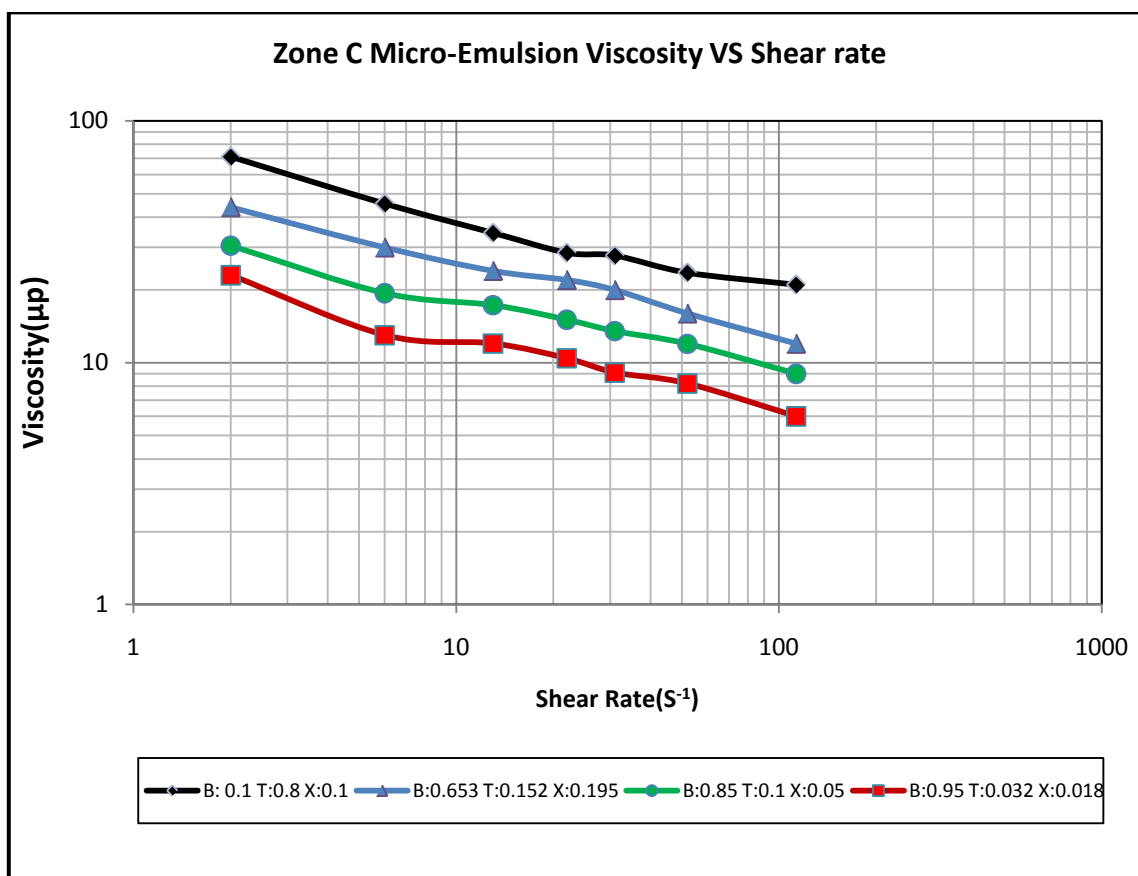


Fig. 4.7 Rheology study results of Zone C micro-emulsions

4.2.3 Emulsion and Crude Oil Interfacial Tension Measurement

Many publications have pointed out that micro-emulsions could provide the ultra-low interfacial tension (IFT) which is welcome in the chemical EOR process. Most of the micro-emulsions used in this research showed very lower IFT, confirming the typical behavior of micro-emulsions. If the micro-emulsion surfactant concentration exceeds the Triton-X 100 critical micelle concentration, the measured interfacial tension between the crude oil and micro-emulsion would be same.

Based on the phase behavior and rheology investigation, Zone-C micro-emulsion, which brine solution is the main composition, could become an ideal emulsion flooding candidate. In particular, the micro-emulsion in the ternary diagram right corner would provide maximum brine concentration and thus cheapest to produce. Then the research focused on Zone-C micro-emulsion. First, **Table 4.1** shows the crude oil interfacial tension measurement results.

Table 4.1 Crude oil interfacial tension measurement (77°F, 14.7 psi)

	Brine(10000ppm NaCl)	Air
Oil	28.9 mN/m	27.5mN/m

Then, from the practical and economical point of view, the optimized micro-emulsion used in the core flooding experiments contains 95wt% brine, 1.8wt% solvent and 3.2wt% surfactant. The micro-emulsion can provide very low interfacial tension with the crude

oil compared with the interfacial tension between 0.5wt% surfactant solution and crude oil which is 1.2mN/m. See **Table 4.2**.

The micro-emulsion sample is showed in the following picture. See **Fig.4.8**.

The viscosity measurement result is presented in **Fig.4.9**.

Table 4.2 Optimized micro-emulsion interfacial tension measurement

	Air	Crude Oil
Micro-emulsion	2.2mN/m	0.08mN/m



Fig. 4.8 Sample of the optimized micro-emulsion.

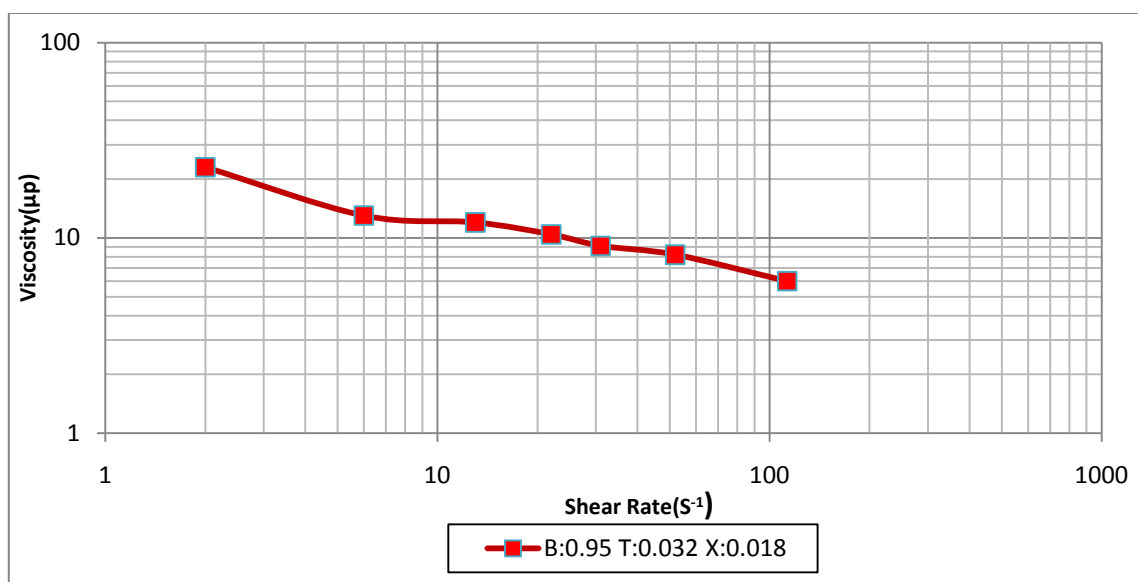


Fig. 4.9 Viscosity measurement of the optimized micro-emulsion

4.2.4 Nanoparticle Thickened Micro-emulsion Experiments

Nanoparticles can also stabilize the emulsion since the huge surface area can provide lower interfacial tension with immiscible phases. And the nano-magnitude of the nanoparticles is two or three orders smaller than the pore throat which makes the nanoparticles stabilized emulsion long-distance migration in the reservoir feasible. Otherwise, there are two advantages in this research by using nanoparticles. Firstly, the nanoparticles can improve the mobility of the emulsion by thickening it. Secondly, the nanoparticles can reduce the surfactant absorption by the porous media and indirectly reduce the usage of the surfactant in the whole chemical enhanced oil recovery process.

In this experiment, the rheology study on the emulsion by adding different amount of nanoparticles had been performed. The results show that the emulsion viscosity increases with increasing amount of the nanoparticles and the emulsion tends to behave

like a Newtonian fluid. Also, the property of the nanoparticles stabilized solvent based emulsion hints that a high apparent viscosity displacing fluid can be attained by adjusting the nanopartilces concentration which is a relatively cheap way.

Fig.4.10 shows the experimental results of the emulsion viscosity measurement by adding different amount of nanoparticles. After adding 0.2g, 0.5g and 1.0g nanoparticles into three glass tubes which contain 10g optimized micro-emulsion, then the tubes were put in the ultrasonic tub for 20mins to form emulsion. Finally, the sample of this kind emulsion had been tested.

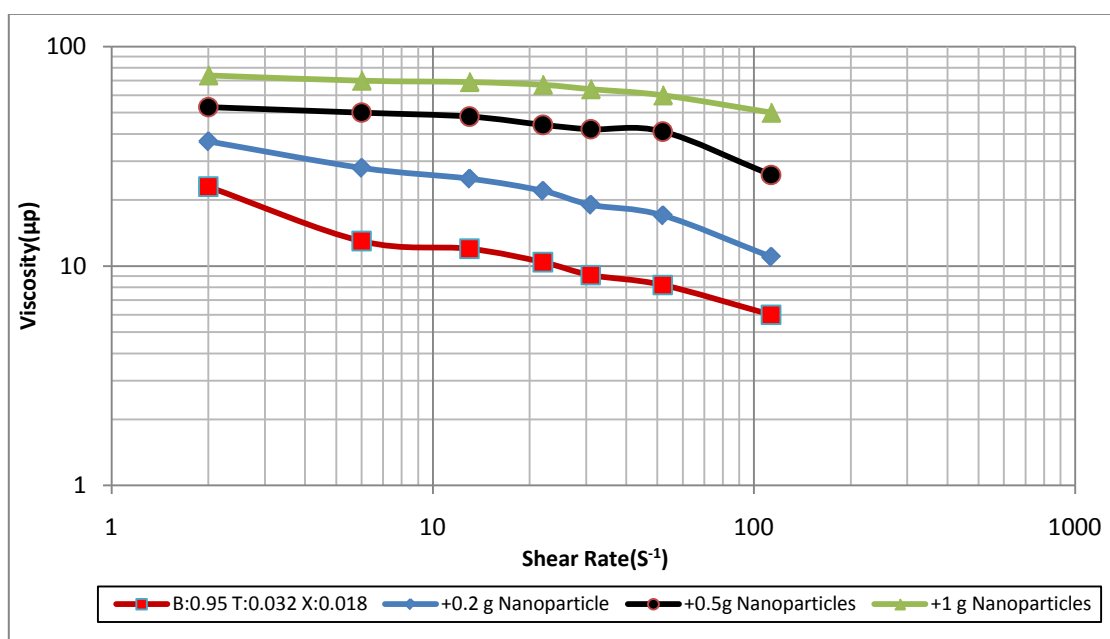


Fig. 4.10 Effect of nanoparticles on the emulsion rheology behavior

4.2.5 Crude Oil Emulsion Viscosity Reduction Experiment

The formation of crude oil in water emulsion could help reduce the reservoir fluid viscosity and then improve the production behavior. The purpose of the experiments is to verify that the solvent existing in the micro-emulsion and the oil in water emulsifier could help to decrease the heavy oil viscosity. The produced effluent in the core flooding experiment may be the crude oil emulsion formed by the injected micro-emulsion and the residual heavy oil.

Fig.4.11 shows results of the experiments. By mixing the crude oil and the optimized micro-emulsion at 1:5 (oil: emulsion) volume ratio, results indicate the apparent viscosity of the crude oil emulsion is reduced from 400 cp to 45 cp generally.

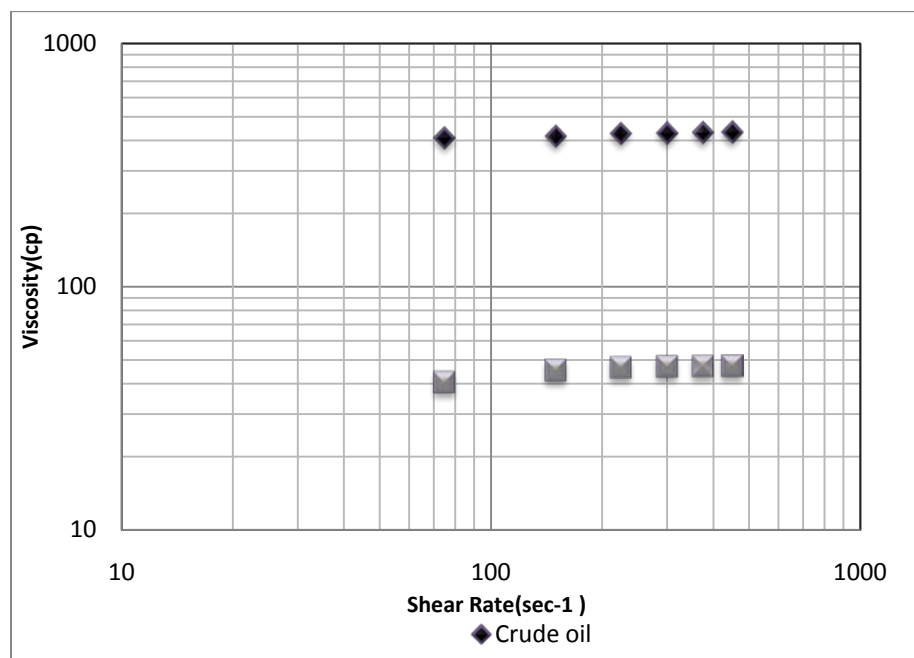


Fig. 4.11 Viscosity reduction of the crude oil

Fig 4.12 shows the crude oil emulsion picture under the microscope which indicates the formation of the oil in water emulsion. The oil in water emulsion has the potential to reduce the apparent viscosity of the heavy oil.

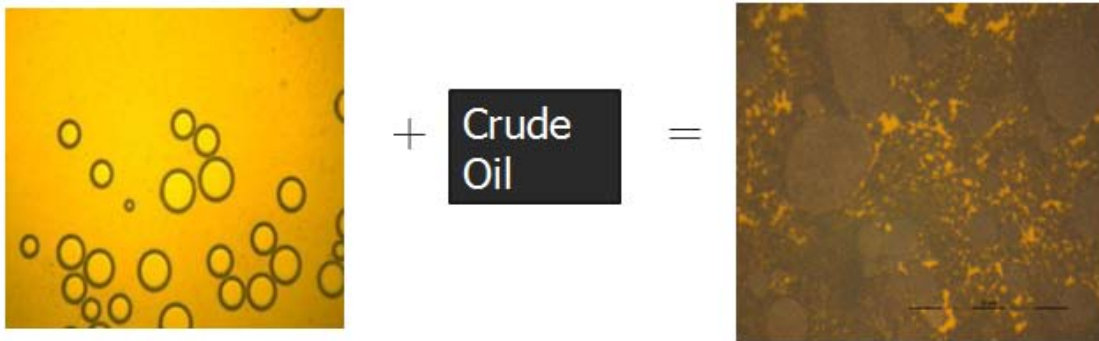


Fig. 4.12 Emulsion pictures under the microscope

Fig.4.13 shows the picture of the crude oil emulsion mixing with micro-emulsion at 1 to 5 volume ratio.



Fig. 4.13 Picture of the crude oil emulsion

4.2.6 Core Flooding Experiments

The core flooding experiments are the final step of this research. These experiments are run to verify the emulsion flooding mechanism discussed in the previous sections and also to evaluate the flooding recovery efficiency under emulsion flooding.

A total of four core-flood experiments were successfully carried out. Two different kinds of sandstone cores were used: Buff Berea sandstone and Idaho sandstone. Buff Berea core permeability is around 200 md and Idaho core permeability is around 800 md. Two different flooding methods were performed on each core in order to make comparisons. The first method involves emulsion flooding after water flooding, while the second method involves pure emulsion flooding.

The injected emulsion also contains the nanoparticles for viscosity control purposes. The nanoparticles make up 4.76wt% of the whole emulsion weight which could thicken the emulsion 3 to 8 times and also weaken the shear-thinning effect of the emulsion. The nanoparticles help form more crude oil emulsion when injecting same volume of optimized emulsion.

The emulsion flooding effluent contains two parts based on the observation. Since the injected micro-emulsion has a better mobility control characteristic and the locally formation of the crude oil emulsion could have a high apparent viscosity (even with the injecting emulsion, the crude oil emulsion become thinning.), it could form piston-like flooding at the beginning. This is the reason that some amount of crude oil was produced in the experiment, but the bigger fraction effluent is crude oil emulsion.

Since the most part of fraction of the emulsion flooding effluent is crude oil emulsion which is hard to be separated, then it is difficult to calculate the oil weight exactly. In this case, I suppose that the effluent volume does not change after the formation of the crude oil emulsion. Then I can find the relationship below to calculate the weight of the oil in the crude oil emulsion.

$$\begin{cases} V_{eff} = V_{mic} + V_{oil} & 4.1 \\ V_{eff} \times \rho_{eff} = V_{mic} \times \rho_{mic} + V_{oil} \times \rho_{oil} & 4.2 \\ V_{eff} \times \rho_{eff} = V_{inj_mic} \times \rho_{mic} + M_{inj_oil} - (M_{Core_after_emul} - M_{Core_dry}) & 4.3 \end{cases}$$

V_{eff} : the volume of the effluent, cm^3

V_{mic} : Supposed volume of the microemulsion in effluent, cm^3

V_{oil} : Supposed volume of the oil in effluent, cm^3

M_{ini_oil} : the initial oil weight in place of the core, g

$M_{Core_after_emul}$: the core weight after emulsion flooding, g

M_{Core_dry} : the dry core weight, g

ρ_{eff} : the density of the effluent, g/cm^3

ρ_{mic} : the density of the microemulsion, g/cm^3

ρ_{oil} : the density of the oil, g/cm^3

And the emulsion flooding effluent performs as crude oil emulsion which is not homogenous, and then the density of crude oil emulsion would be hard to be a constant value. However, we can utilize the two materials balance condition of the emulsion flooding effluent to get the oil fraction in the effluent, V_{oil} , then calculate the weight of that.

Case 1: Berea core with water flooding followed by emulsion flooding

Table 4.3 lists the core flooding results based on material balance calculation. The residual oil saturation could be reached after 2.1 PV water injection which recovered 76.2% OOIP heavy oil. Then another 1 PV micro-emulsion was injected and produced additional 19.2% oil in crude oil emulsion.

Table 4.3 Case 1 core flooding experimental results

Dry weight of the Buff Berea sandstone core	308.43g
After water saturation ,the weight of the core	353.33g
Pore Volume	43.24
Porosity	28%
After flooding with oil, the weight of the core	349.96g
Water displaced by heavy oil	34.89g
Irreducible water saturation(S_{wi})	19.28%
Initial oil in place for this core	33.2g
Oil weight after 2.1 PV water injection	25.3g
Oil recovery factor after water flooding	76.20%
Oil weight after 1 PV emulsion injection	6.37g
Oil recovery factor after emulsion flooding	95.40%

Fig.4.14 shows the oil recovery profile for case 1. The emulsion flooding effluent was analyzed at the end of the experiment since most fractions are in crude oil emulsion. Oil fraction in the effluent was calculated by the equation sets mentioned above. Also the effluent was separated in the centrifuge for 1 hour in order to make sure no more crude oil could be separated from the emulsion physically.

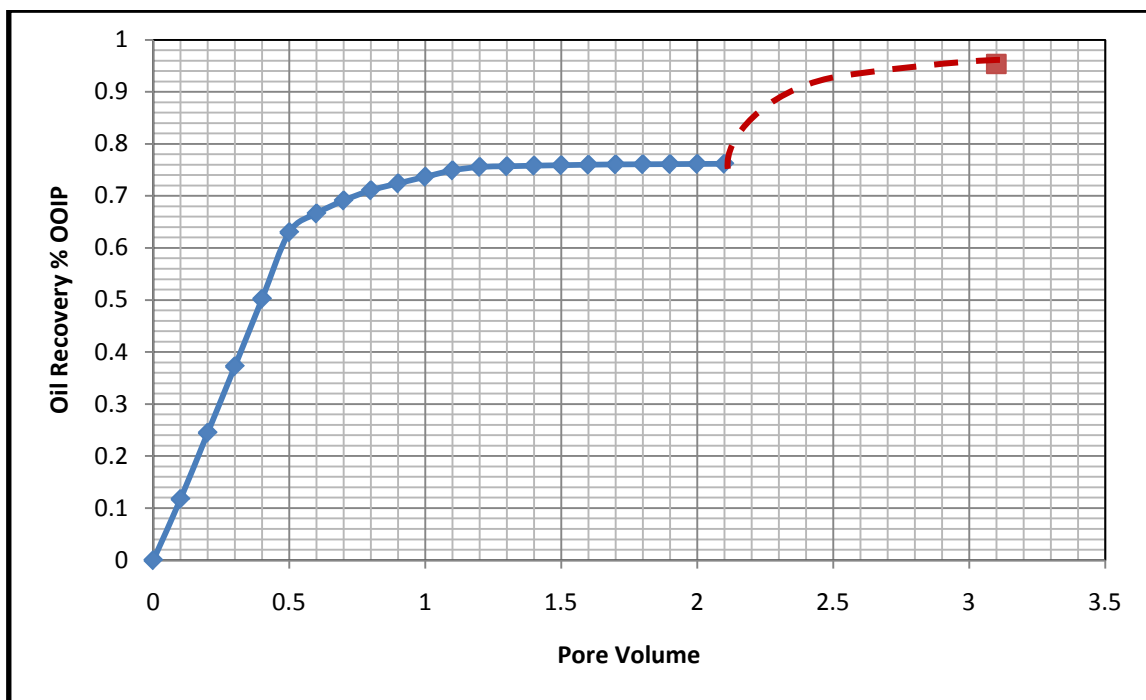


Fig. 4.14 Case 1 core flooding experiment oil recovery profile

Fig.4.15 shows pictures of the effluent of the core flooding experiments. From left to right, we can easily figure out the effect of flooding type on the effluent. As mentioned above, after 2.1 PV water injections, no more oil could be produced and the third tube only shows the produced water. The crude oil emulsion occupied the most volume percentage in the fourth tube.

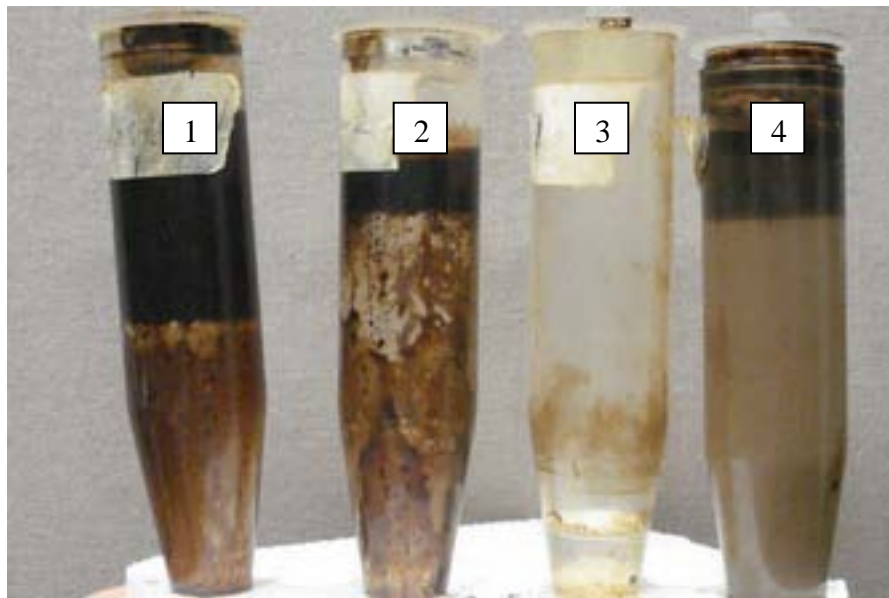


Fig. 4.15 Case 1 core flooding effluent collected in the 50 cc plastic tube.

Fig.4.16 is the pictures of the core at each core flooding stage. The difference in core color indicates the various saturation and flooding stages, the change in color being due to the different fluid type being present in the core.

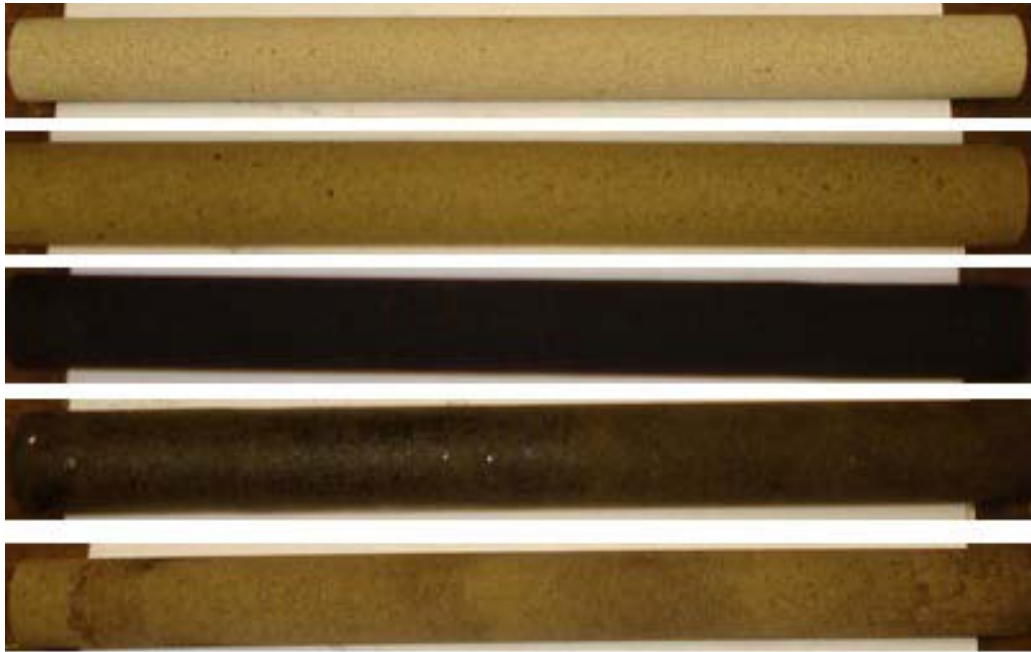


Fig. 4.16 Case 1 core pictures of each core flooding stage

Case 2: Berea core with pure emulsion flooding

The main objectives of pure emulsion flooding are

- (1) to investigate if the piston-like crude oil emulsion flooding could form for a longer time then the breakthrough time point would be later for the same kind of core and
- (2) to evaluate changes in oil recovery.

Table 4.4 lists the core flooding results based on the materials balance calculation in Case 2. The second Berea core has very similar properties to the first Berea core which is necessary for comparisons to be made.

Table 4.4 Case 2 core flooding experiment results

Dry weight of the Buff Berea sandstone core	307.12g
After water saturation ,the weight of the core	352.3g
Pore Volume	43.03cm ³
Porosity	27.86%
After flooding with oil, the weight of the core	346.88g
Water displaced by heavy oil	36.88g
Irreducible water saturation(S_{wi})	18.37%
Initial oil in place for this core	31.46g
Oil weight after 1.6 PV emulsion injection	30.45g
Oil recovery factor after emulsion flooding	96.81%

Fig.4.17 indicates the oil recovery profile of Case 2. Since the injection of micro-emulsion at an earlier time comparing with Case 1, the emulsification of the crude oil and micro-emulsion form a more viscous driving fluid at the interface which leads to the piston-like flooding and also a delayed breakthrough time. The total flooding time IS about 50% of the Case 1 flooding time which means the emulsion flooding is more efficient. A total of 1.6 pore volume micro-emulsions were injected into the core to obtain oil recovery of 96.81% OOIP.

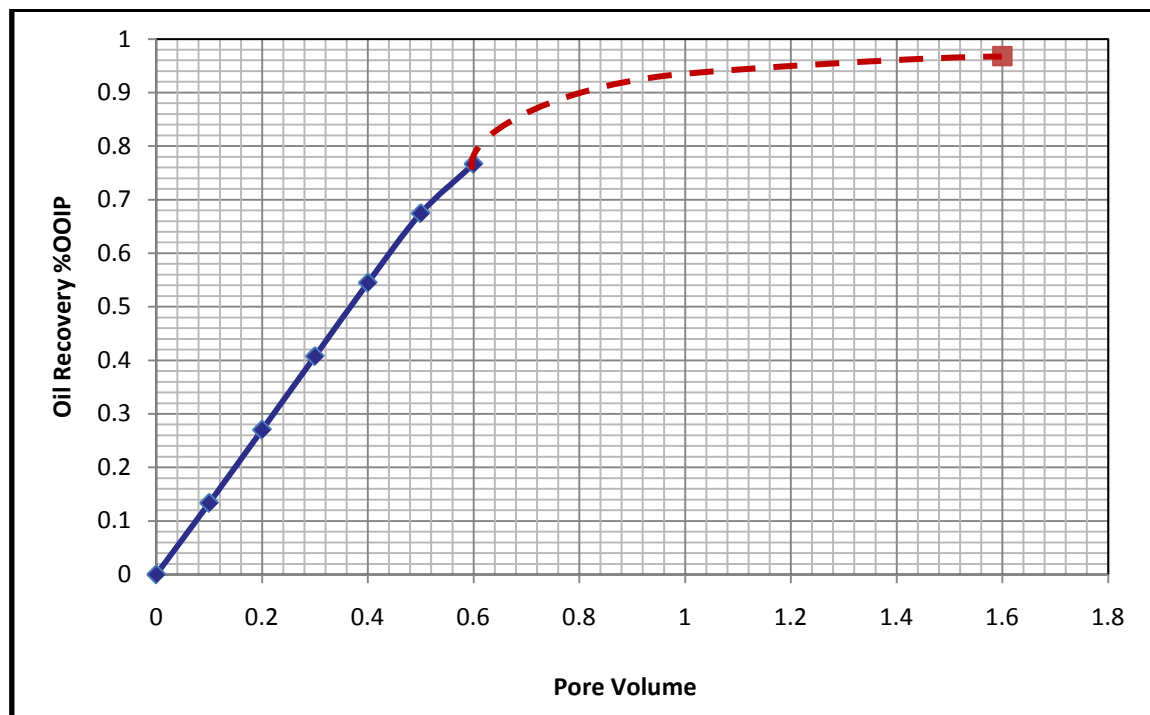


Fig. 4.17 Case 2 core flooding experiment oil recovery profiles

Fig.4.18 shows pictures of the effluent for Case 2 core flooding run. The collection of the effluent in the left tube shows about 23.2 cm^3 crude oil which is not emulsion. This comes at the beginning of the flooding. Then the crude oil emulsion was produced thereafter.



Fig. 4.18 Case 2 core flooding effluent collected in the 50 cc plastic tube.

Fig.4.19 shows pictures of the core for the run in the Case 2, indicating each core flooding stage. The core color changes according to the fluid type contained in the core.



Fig. 4.19 Case 2 core pictures of Case 2 core flooding stage

Case 3: Idaho Core with water flooding followed by emulsion flooding

The Idaho core is more permeable than the Berea core. The air permeability is 800 mD. **Table 4.5** shows the core flooding results of Case 3. The residual oil saturation could be reached after about 1.2 PV water injections which recovered 56.2% OOIP heavy oil.

Table 4.5 Case 3 core flooding experiment results

Dry weight of the Buff Berea sandstone core	276.94g
After water saturation ,the weight of the core	322.26g
Pore Volume	43.16cm ³
Porosity	27.95%
After flooding with oil, the weight of the core	307.84g
Water displaced by heavy oil	34.11g
Irreducible water saturation(S_{wi})	24.74%
Initial oil in place for this core	30.90g
Oil weight after 1.2 PV water injection	17.37g
Oil recovery factor after water flooding	56.2%
Oil weight after 1 PV emulsion injection	8.16g
Oil recovery factor after emulsion flooding	82.6%

Fig. 4.20 illustrates the oil recovery profile of Case 3. Since the high permeability of the core, the water channels or viscous fingers were formed easily than in Case 1 under water flooding condition. The water flooding oil recovery factor is much lower than that in Case 1. But it also provides the chance to show the advantages of the emulsion flooding, since much more bypassed heavy oil was left by water flooding, the formation of the crude oil emulsion resulted in additional 26.4% OOIP recovery in this case. A total of 1 PV micro-emulsion was injected into the core.

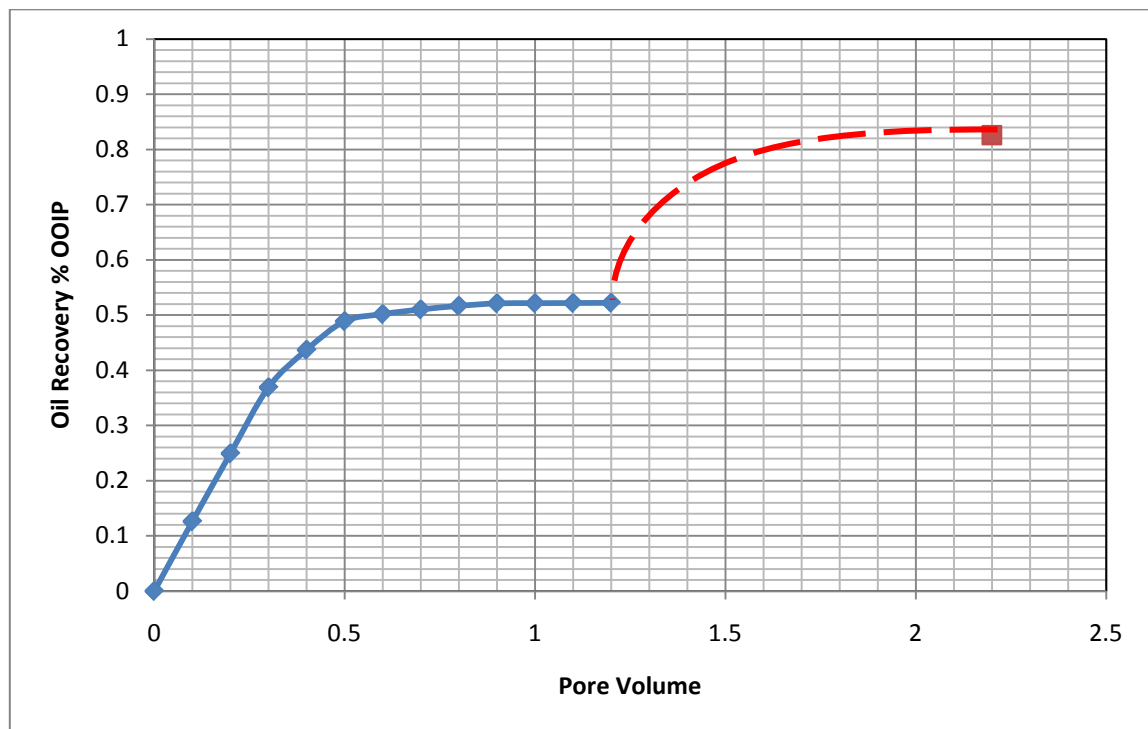


Fig. 4.20 Case 3 core flooding experiment oil recovery profiles

Fig.4.21 shows pictures of the effluent for Case 3 core flooding run.



Fig. 4.21 Case 3 core flooding effluent collected in the 50 cc plastic tube.

Fig.4.22 shows Case 3 core pictures of each flooding stage. Simply, the core color changes indicate the flooding experimental stages and recovery effects.



Fig. 4.22 Case 3 core pictures of each flooding stage

Case 4: Idaho core with pure emulsion flooding

The shear rate of the fluid flowing in Idaho core is lower than that for the Berea core due to the permeability, so the emulsification of the crude oil emulsion in Idaho core would be more difficult than that in the Berea core. See **Table 4.6**.

Table 4.6 Case 4 core flooding experiment results

Dry weight of the Buff Berea sandstone core	278.58g
After water saturation ,the weight of the core	323.77g
Pore Volume	43.04cm ³
Porosity	28%
After flooding with oil, the weight of the core	320.69g
Water displaced by heavy oil	33.98g
Irreducible water saturation(Swi)	24.8%
Initial oil in place for this core	30.9g
Oil weight after 1.4 PV emulsion injection	26.51g
Oil recovery factor after emulsion flooding	85.8%

Fig.4.23 illustrates the oil recovery profile of Case 4. After the piston-like flooding at the beginning, the formations of the crude oil emulsion resulted in additional oil recovery. A total of 1.4 pore volume micro-emulsion was injected into the core and 85.8% OOIP was recovered which is more than that for Case 3.

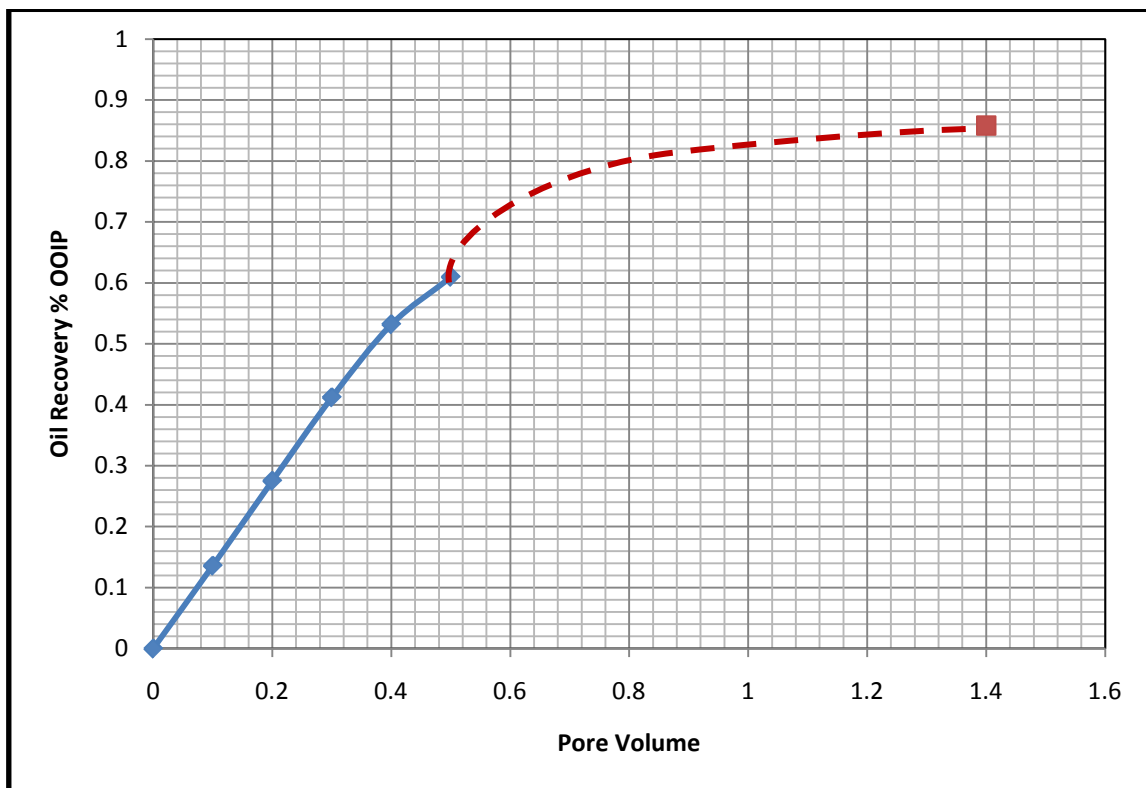


Fig. 4.23 Case 4 core flooding experimental oil recovery profiles

Fig.4.24 shows pictures of the effluent collected in the Case 4 core flooding run.



Fig. 4.24 Case 4 core flooding effluent collected in the 50 cc plastic tube.

Fig.4.25 shows the Case 4 core pictures of each flooding stage.



Fig. 4.25 Case 4 core pictures of each flooding stage

4.2.7 Comparison of Experimental Results

We compared the recovery profiles for all the cases to investigate the effectiveness or efficiency of the emulsion flooding and the permeability effect on the emulsion flooding.

Fig.4.26 shows that the pure emulsion flooding (Case 2) provides a better sweep efficiency than water flooding followed by emulsion flooding (Case 1) at the beginning. The piston-like flooding also delays the breakthrough time for Case2. After the breakthrough, one more pore volume micro-emulsion was injected into the core and the ultimate recovery factor of case 2 is higher than that of case 1.

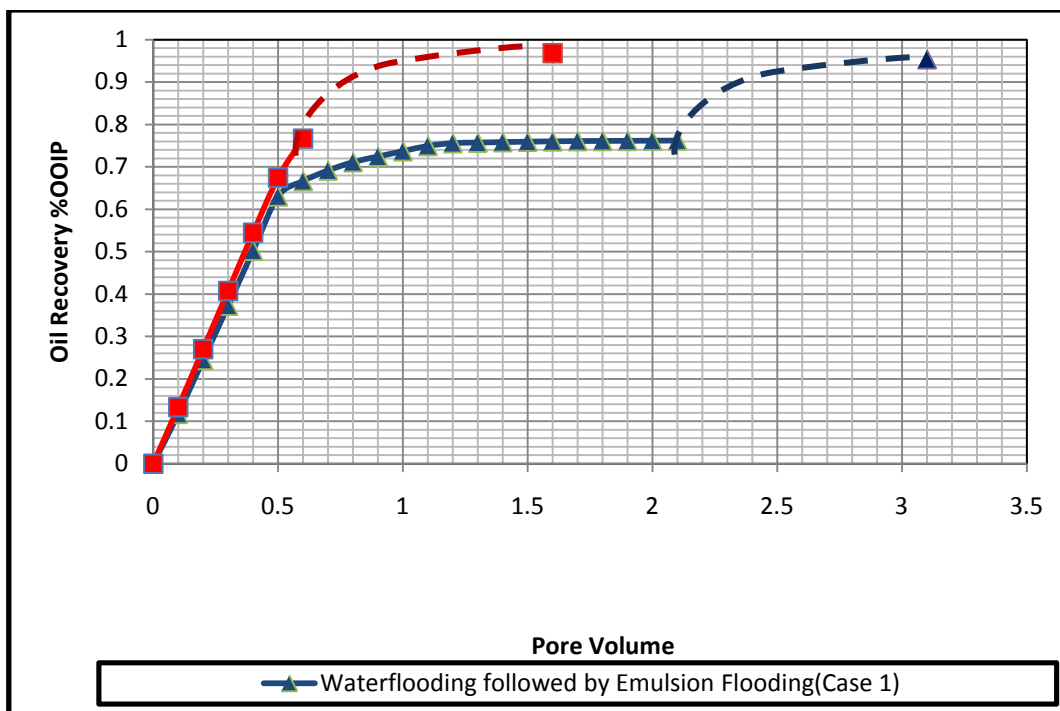


Fig. 4.26 Comparisons of the Berea core flooding experiment results

Fig. 4.27 shows that the pure emulsion flooding (Case 4) results in better recovery efficiency than water flooding followed by emulsion flooding (Case 3) at the beginning. The piston-like flooding also delays the breakthrough time in Case 4. After the breakthrough, one more pore volume micro-emulsion was injected into the core and the resulting ultimate oil recovery factor of case 4 is higher than that of Case 3.

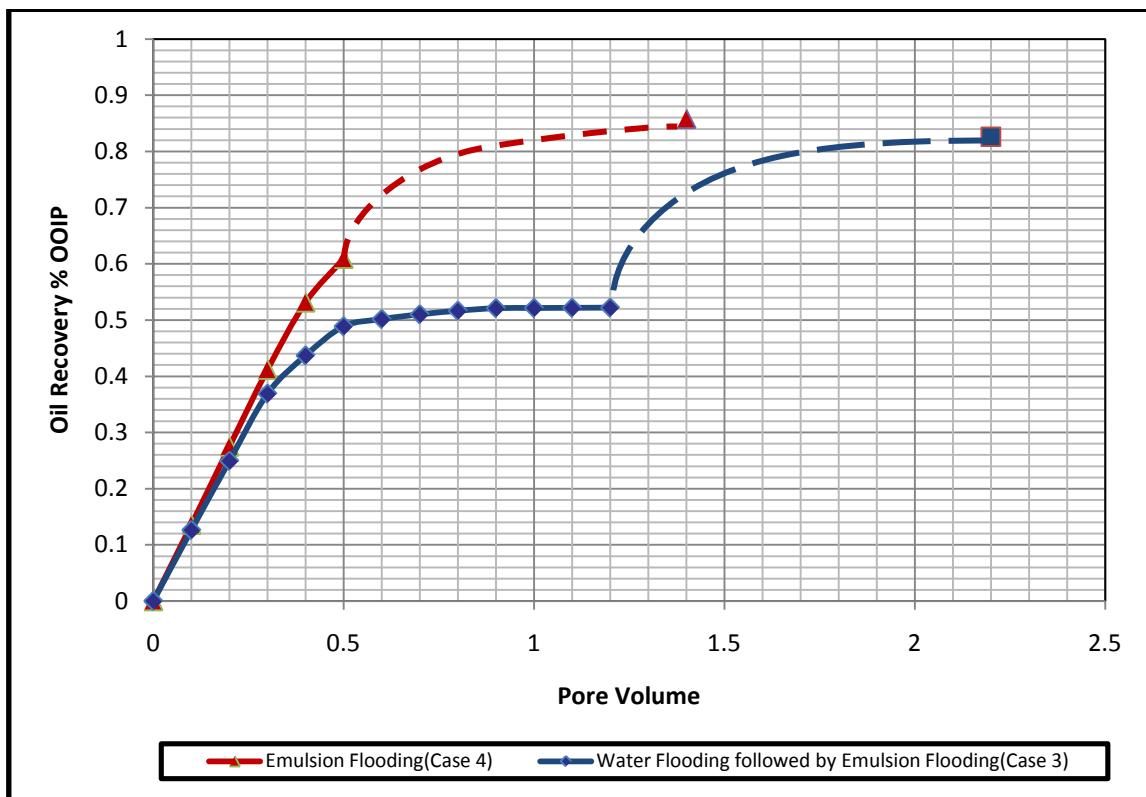


Fig. 4.27 Comparison of the Idaho core flooding experimental results

The significant differences in the permeability of cores lead to the difference in the oil recovery factor. As mentioned above, the fluid flowing in the high permeability core more readily forms severe water channel than in lower permeability cores, resulting in more bypassed oil than in lower permeability cores. This would also lead earlier breakthrough time. Also, the shear rate of fluid flowing in Idaho core is lower than that in Berea core and then the emulsification of the crude oil may be not sufficient. Finally, the oil recovery factor in the Idaho core flooding runs is smaller than that for the Berea core flooding runs.

Fig 4.28 shows the oil recovery profile comparison between Case 1 and Case 3.

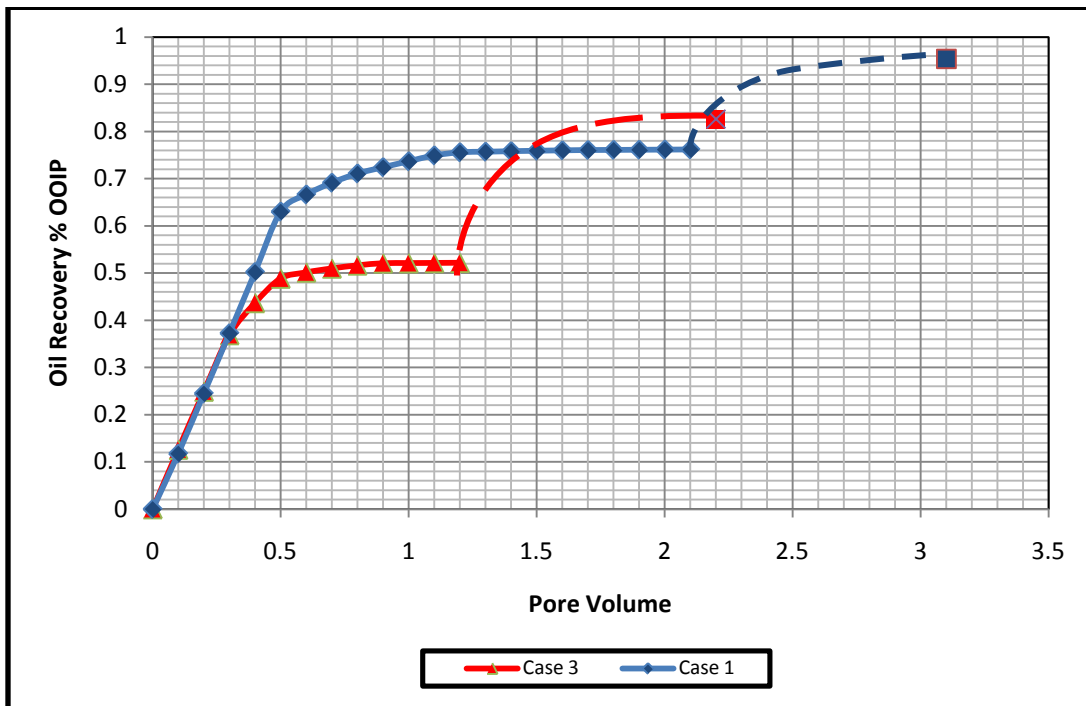


Fig. 4.28 Core flooding oil recovery profile comparison between Case 1 and Case 3

Fig.4.29 shows the recovery profile comparison between Case 2 and Case 4.

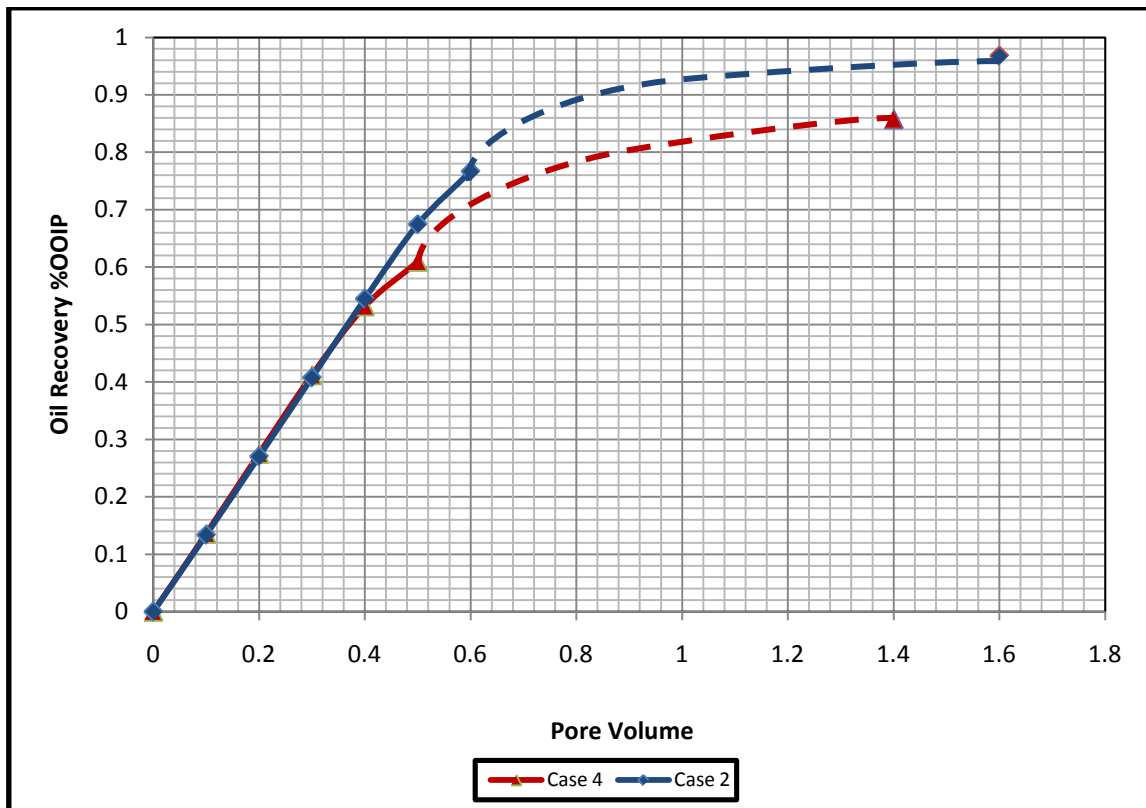


Fig. 4.29 Core flooding oil recovery profile comparison between Case 2 and Case 4

5. SUMMARY, CONCLUSIONS AND RECOMMENDATIONS

5.1 Summary

The main thrust of the research was to evaluate the potential application of nano-particle-stabilized solvent base emulsion injection to enhance heavy oil recovery in the Alaska North Slope area. Bench tests including phase behavior scan, rheology study, and interfacial tension measurement were used to optimize the possible micro-emulsion composition subjected to the technical and economical consideration. A stable micro-emulsion containing 90.48wt% brine, 1.71wt% solvent, 3.05wt% surfactant and 4.76wt% nano-particles were chosen for the core flooding experiments.

Four successful core flood experiments were performed using heavy oil from the West Sak oil field in Alaska North Slope area. Two different kinds of cores, namely, Berea core and Idaho core were used for the coreflood experiments. The runs made were (1) water flooding followed by emulsion flooding and (2) pure emulsion injection core flooding. During the experimental runs, the following conditions were kept constant: injection rate (0.5cc/min) and core flooding temperature (77F) and only 1 PV micro-emulsion was injected after breakthrough under water flooding or emulsion flooding.

5.2 Conclusions

The following main conclusions may be drawn from the experimental results:

1. A micro-emulsion will form if the surfactant concentration reaches a critical value in the emulsion system. In this case, Triton X-100 concentration does not surpass the 10wt% of the total mass to form micro-emulsion. It is possible to form micro-

emulsion with low surfactant concentration. Based on the ternary phase behavior diagram, the optimum micro-emulsion without nano-particles used in the core flood experiments contains 95wt% brine, 1.8wt% solvent, 3.2wt% surfactant.

2. Addition of nano-particles to the micro-emulsion increases the viscosity of the micro-emulsion, resulting in a favorable mobility ratio at the beginning of the injection. Nano-particles also help to make in situ crude oil emulsification which could mobilize the bypassed heavy oil and form a favorable miscible flooding recovery process.
3. The optimized micro-emulsion provides an ultra-low interfacial tension (0.08mN/m) between micro-emulsion and West Sak heavy oil which is desired to form continuous emulsion flooding.
4. The experiments involving mixing by the optimized micro-emulsion and West Sak crude oil, indicated the viscosity reduction mechanisms to be solvent dissolving oil and formation of oil in water emulsion.
5. In the Berea core flood experiments, emulsion flooding increased the oil recovery factor by 19.2 points after water flooding (from 76.2% to 95.4% OOIP). This indicates that the bypassed crude oil in situ emulsification probably blocked the water channels, increasing the sweep efficiency and also mobilized the residual crude oil. Oil recovery with pure emulsion flooding was 96.8% OOIP. This recovery is slightly higher than that with water flooding followed by emulsion flooding, 95.4% OOIP, probably because of the delayed breakthrough time caused by formation of a more viscous crude oil emulsion.

6. In the Idaho core flood run, due to the high permeability of the core compared to that of Berea core, the breakthrough time is earlier than for the Berea core flood runs. More bypassed oil is left behind at the end of water flooding. The same pore volume emulsion flooding behaves more effectively than for Berea core flood runs. Oil recovery increased by 26.4 percent points from 56.2% OOIP with waterflooding to 82.6% OOIP with injection of emulsion following waterflooding. With pure emulsion flooding, oil recovery is slightly higher at 85.8% OOIP.
7. Low permeability typically results in a higher shear rate which is favorable for the in situ emulsification and higher displacement efficiency. This is verified by comparing the emulsion flooding oil recovery profiles for the two different cores.

5.3 Recommendations

1. More core flooding experiments should be made to more accurately determine the optimum the micro-emulsion concentration.
2. Depending on the crude oil properties, a specific surfactant is required to maximize the advantage of emulsion flooding
3. Consider the use of other kinds of solvents to satisfy the environmental issues related to xylene.

REFERENCES

- Bouabboune, M., Hammouch, N., & Benhadid, S., 2006. Comparison Between Micro-Emulsion and Surfactant Solution Flooding Efficiency for Enhanced Oil Recovery in TinFouye Oil Field. Paper presented at the Canadian International Petroleum Conference. SPE 2006-058.
- Bryan, J. L., & Kantzas, A., 2007. Enhanced Heavy-Oil Recovery by Alkali-Surfactant Flooding. Paper presented at the SPE Annual Technical Conference and Exhibition. SPE 110738-MS
- Bryan, J. L., Mai, A. T., & Kantzas, A., 2008. Investigation into the Processes Responsible for Heavy Oil Recovery by Alkali-Surfactant Flooding. Paper presented at the SPE/DOE Symposium on Improved Oil Recovery. SPE 113993-MS
- Flaaten, A., Nguyen, Q. P., Pope, G. A., & Zhang, J., 2008. A Systematic Laboratory Approach to Low-Cost, High-Performance Chemical Flooding. Paper presented at the SPE/DOE Symposium on Improved Oil Recovery. SPE 113469-MS
- Healy, R. N., Reed, R. L., 1974. Physicochemical Aspects of Microemulsion Flooding. 14(5), 491-501. SPE 4583-PA
- Healy, R. N., Reed, R. L., Carpenter Jr., C. W., 1975. A Laboratory Study of Microemulsion Flooding (includes associated papers 6395 and 6396). 15(1), 87-103. SPE 4752-PA
- Mai, A., Bryan, J., Goodarzi, N., & Kantzas, A., 2009. Insights into Non-Thermal Recovery of Heavy Oil. 48(3). SPE 09-03-27
- Seright, R. S., 2006. Cleanup of Oil Zones after a Gel Treatment. SPE Production & Operations, 21(2), 237-244.
- Thomas, 2007. Enhanced Oil Recovery - An Overview. Oil & Gas Science and Technology, 63(January-February 2008), 9-19.
- Willhite, G. P., Green, D. W., Okoye, D. M., & Looney, M. D., 1980. A Study of Oil

Displacement by Microemulsion Systems Mechanisms and Phase Behavior. SPE Journal, 20(6), 459-472.

Zhang, T., Roberts, M., Bryant, S. L., & Huh, C., 2009. Foams and Emulsions Stabilized with Nanoparticles for Potential Conformance Control Applications. Paper presented at the SPE International Symposium on Oilfield Chemistry. SPE 121744-MS

APPENDIX

Table A1- Ternary phase diagram data

Water (wt %)	Tx-100(wt %)	Xylene(wt %)
0.05	0.04	0.91
0.074	0.048	0.878
0.0789	0.052	0.8691
0.0815	0.054	0.8645
0.086	0.055	0.859
0.088	0.06	0.852
0.093	0.062	0.845
0.11	0.065	0.825
0.112	0.068	0.82
0.12	0.069	0.811
0.13	0.07	0.8
0.134	0.072	0.794
0.139	0.074	0.787
0.142	0.076	0.782
0.15	0.079	0.771
0.157	0.08	0.763
0.161	0.082	0.757
0.1685	0.0825	0.749
0.179	0.083	0.738
0.188	0.0839	0.7281
0.197	0.0842	0.7188
0.2089	0.085	0.7061
0.219	0.0852	0.6958
0.2276	0.0864	0.686
0.234	0.087	0.679
0.2476	0.0874	0.665
0.259	0.088	0.653
0.2647	0.0883	0.647
0.273	0.0884	0.6386
0.288	0.0885	0.6235
0.296	0.0886	0.6154
0.305	0.0887	0.6063
0.321	0.09	0.589

0.34	0.092	0.568
0.3609	0.0921	0.547
0.3828	0.0922	0.525
0.398	0.093	0.509
0.4178	0.0932	0.489
0.4249	0.0941	0.481
0.438	0.095	0.467
0.4548	0.0952	0.45
0.4805	0.0955	0.424
0.4944	0.0956	0.41
0.501	0.0957	0.4033
0.51	0.0958	0.3942
0.52	0.0959	0.3841
0.525	0.096	0.379
0.5392	0.0958	0.365
0.5467	0.0957	0.3576
0.556	0.0956	0.3484
0.566	0.0955	0.3385
0.5756	0.0954	0.329
0.5847	0.0953	0.32
0.599	0.0952	0.3058
0.61	0.0951	0.2949
0.612	0.095	0.293
0.632	0.094	0.274
0.658	0.092	0.25
0.679	0.091	0.23
0.699	0.09	0.211
0.71	0.087	0.203
0.72	0.084	0.196
0.731	0.081	0.188
0.754	0.078	0.168
0.774	0.074	0.152
0.78	0.071	0.149
0.798	0.07	0.132
0.805	0.068	0.127
0.812	0.065	0.123
0.82	0.06	0.12
0.835	0.058	0.107
0.85	0.055	0.095

0.87	0.052	0.078
0.888	0.05	0.062
0.9	0.047	0.053
0.905	0.045	0.05
0.924	0.041	0.035
0.938	0.038	0.024
0.945	0.034	0.021
0.95	0.03	0.02

VITA

Name: Fangda Qiu

Permanent address: 3116 TAMU, Richardson Building
Texas A&M University, College Station, Texas, 77843

Education: B.S. Petroleum Engineering
China University of Petroleum, Beijing, China 2008
M.S. Petroleum Engineering
Texas A&M University, College Station 2010

Member: Society of Petroleum Engineers

Email address: qiufangda@gmail.com